



## Geodesic Active Regions and Level Set Methods for Supervised Texture Segmentation\*

NIKOS PARAGIOS

*Imaging and Visualization Department, Siemens Corporate Research, Princeton, NJ 08540, USA*

nikos@scr.siemens.com

RACHID DERICHE

*Computer Vision and Robotics Group (RobotVis), I.N.R.I.A. Sophia Antipolis, 06902, France*

der@sophia.inria.fr

*Received November 5, 1998; Revised August 30, 2001; Accepted September 28, 2001*

**Abstract.** This paper presents a novel variational framework to deal with frame partition problems in Computer Vision. This framework exploits boundary and region-based segmentation modules under a curve-based optimization objective function. The task of supervised texture segmentation is considered to demonstrate the potentials of the proposed framework. The textured feature space is generated by filtering the given textured images using isotropic and anisotropic filters, and analyzing their responses as multi-component conditional probability density functions. The texture segmentation is obtained by unifying region and boundary-based information as an improved Geodesic Active Contour Model. The defined objective function is minimized using a gradient-descent method where a level set approach is used to implement the obtained PDE. According to this PDE, the curve propagation towards the final solution is guided by boundary and region-based segmentation forces, and is constrained by a regularity force. The level set implementation is performed using a fast front propagation algorithm where topological changes are naturally handled. The performance of our method is demonstrated on a variety of synthetic and real textured frames.

**Keywords:** supervised texture segmentation, Gabor filters, mixture analysis, Geodesic Active Contours, propagation of curves, level set methods

### 1. Introduction

Frame partition problems are among the most important problems in many image analysis and computer vision applications. This article provides a general frame partition variational and level-set based framework that integrates boundary and region-based seg-

mentation information and apply it to the problem of texture segmentation. In this application, the task is to partition the image into a number of regions such that each region has the same textural properties (Jain and Farrokhnia, 1991; Manjunath and Chellapa, 1991b; Jain and Bhattacharjee, 1992; Zeng et al., 1998). Alternatively, this task can be viewed as the problem of accurately extracting the borders between different texture regions in an image (Khotanzand and Chen, 1989; Manjunath and Chellapa, 1991a). If a priori knowledge regarding the textural properties in a given image is available, the problem is called supervised texture segmentation; otherwise it is called un-supervised.

\*This work has been carried out during the appointment (doctoral research) of the first author with the Computer Vision and Robotics Group (RobotVis) of I.N.R.I.A. Sophia Antipolis from October 1, 1996 to November 1, 1999 and was funded in part under the VIRGO research network (EC Contract No ERBFMRX-CT96-0049) of the TMR Program.

In this paper, we apply our variational and level-set based framework to the problem of supervised texture segmentation where the first step is texture analysis and modeling, usually referred as *learning phase*. The texture analysis requires the identification of proper attributes, features or textural properties that differentiate the textures in the image for segmentation. Alternatively, texture modeling requires the adoption of a general framework capable of describing a wide variety of texture prototypes. Approaches to texture analysis and modeling can be mainly classified into two groups:

- Traditional *statistical modeling* makes the assumption that statistics of each texture are stationary, and is based to the analysis of local spatial interactions (co-occurrence matrices (Elfadel and Picard, 1994), second order statistics (Chen and Pavlidis, 1983), Gauss Markov Random Fields (Cross and Jain, 1983; Mao and Jain, 1992), and local linear transforms (Unser, 1986)).
- *Filtering theory* decomposes the retinal into a set of different sub-bands that are convolved images of the input image with a bank of filters. A quite common filter bank selection is Gabor filters (Gabor, 1946; Bovik et al., 1990; Dunn and Higgins, 1995), or the wavelet transform (Mallat, 1989; Simoncelli et al., 1992) which is usually applied in a pyramid-structure form (Chang and Kuo, 1993; Laine and Fan, 1993; Unser, 1995).

Feature-based image segmentation is performed using two basic image processing techniques: the *boundary-based segmentation* (which is often referred as edge-based) relies on the generation of a strength image and the extraction of prominent edges, while the *region-based segmentation* relies on the homogeneity of spatially localized features and properties.

- Early approaches for *boundary-based* image segmentation have utilized local filtering techniques such as edge detection operators (Canny, 1986; Deriche, 1987). These approaches are a compromise between simplicity, with accompanying light computational cost and stability under noise, but have difficulty in establishing the connectivity of edge segments. This problem has been confronted by employing Snakes/Balloons/Deformable Templates (Kass et al., 1988; Cohen, 1991; Blake and Isard, 1997) which can provide a closed curve as a compromise between regularity of the curve and high

gradient values among the curve points. The main handicap of these approaches is that they require a good initialization step. Recently, a new active contour model has been introduced (Caselles et al., 1995; Kichenassamy et al., 1995; Malladi et al., 1995; Sapiro, 1996) that presents some quite nice properties. The initialization step doesn't impose any significant constraint, while new techniques are proposed for the curve propagation (level-set methods (Osher and Sethian, 1988)), which can deal successfully with topological changes (merging and splitting). Although for many real cases the use of boundary-based segmentation methods are inappropriate, they present some important advantages. Shape variations are naturally handled and they are not sensitive to global illumination changes due to the fact that they rely on relative illumination changes, rather than the absolute illumination intensities. Additionally, these methods require low computational cost and localize better the region/object boundaries. There is a limited set of boundary-based approaches for texture segmentation (Manjunath and Chellapa, 1991a; Jones, 1994; Yhann and Young, 1995; Ma and Manjunath, 1997; Solloway et al., 1997; Kapur et al., 1998; Lorigo et al., 1998; Zeng et al., 1998), since the detection of edges in textured images is a tougher task, due to the fact that the textural boundaries are difficult to locate.

- The *region-based* segmentation techniques are more suitable for segmenting the textured images and can be roughly classified into two categories: The region-growing techniques has been widely used (Chen and Pavlidis, 1979; Raafat and Wong, 1988; Reed et al., 1990; Adams and Bischof, 1994; Leonardis et al., 1995). They are usually based on split-and-merge procedures using statistical homogeneity tests, where the statistics are generated and updated dynamically, while the manner with which initial regions are formed and the criteria for splitting and merging them are set a priori. The resulting segmentation will inevitably depend on the choice of initial regions, while irregularities on the boundaries will appear since the region shapes depend on the particular growing algorithm. Another powerful region-based tool, which has been widely investigated for texture segmentation, is the Markov Random Fields (Geman and Geman, 1984). In that case the segmentation problem is viewed as a statistical estimation problem where each pixel is statistically dependent only on its neighbors so that the complexity

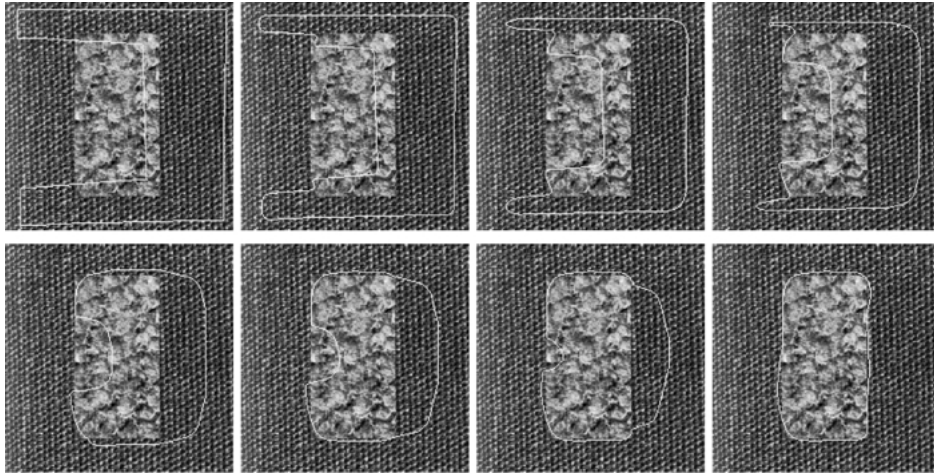


Figure 1. Geodesic Active Regions for supervised texture segmentation: A curve is initialized in a textured image (top-left). The proposed framework propagates this curve towards the final segmentation map that separates the background textured region from the other textured regions (bottom-right).

of the model is restricted. The segmentation is obtained by finding the maximum *a posteriori* map given the observed data (Cross and Jain, 1983; Derin and Eliot, 1987; Bouman and Liu, 1991; Manjunath and Chellapa, 1991b; Jain and Farrokhnia, 1991; Elfadel and Picard, 1994; Chen and Kundu, 1995; Panjwani and Healey, 1995; Raghu and Yegnanarajana, 1996). The main advantage of this type of approaches is that they are less affected from the presence of noise, and provide a global segmentation criterion. However, the resulting objective function of the *MAP* estimate is quite difficult to be globally maximized, which is considered as a significant drawback.

Besides, there is a significant effort to *integrate boundary-based with region-based segmentation approaches* (Haddon and Boyce, 1990; Pentland, 1990; Leonardis et al., 1995; Chakraborty et al., 1996; Zhu and Yuille, 1996; Siddiqi et al., 1997). The difficulty lies on the fact that even though the two modules yield complementary information, they involve conflicting and incommensurate objectives. The region-based methods attempt to capitalize on homogeneity properties, whereas boundary-based ones use the non-homogeneity of the same data as a guide.

This article is focusing on two objectives. The first and main objective is to provide a general frame-partition variational framework<sup>1</sup> (*Geodesic Active Regions*) that integrates boundary and region-based

segmentation modules, is free from the initial conditions, can deal automatically with topological changes and can be used to deal with various frame partition problems.

The second is to validate this framework using a well known application in Computer Vision, the task of supervised texture segmentation. The observation set of the proposed approach is composed of

1. A given set of texture pattern images,
2. A given input frame composed from these patterns.

Based on this feature space, a simple method is proposed for texture analysis and modeling that combines efficiently filtering theory with the statistical modeling. Then, the boundary and the region-based texture segmentation modules are integrated under a generic form within the Geodesic Active Regions model to deal with the following problems (Paragios and Deriche, 1999a, 1999b):

1. The *segmentation of the input frame*, given the background pattern (Figs. 1, 11 and 14),
2. The extraction of *regions of interest* from the input frame, given the corresponding patterns (Figs. 12 and 13).

The essence of our approach is demonstrated in Fig. 1 where an initial contour is propagated towards the boundaries of the region of interest provide the final

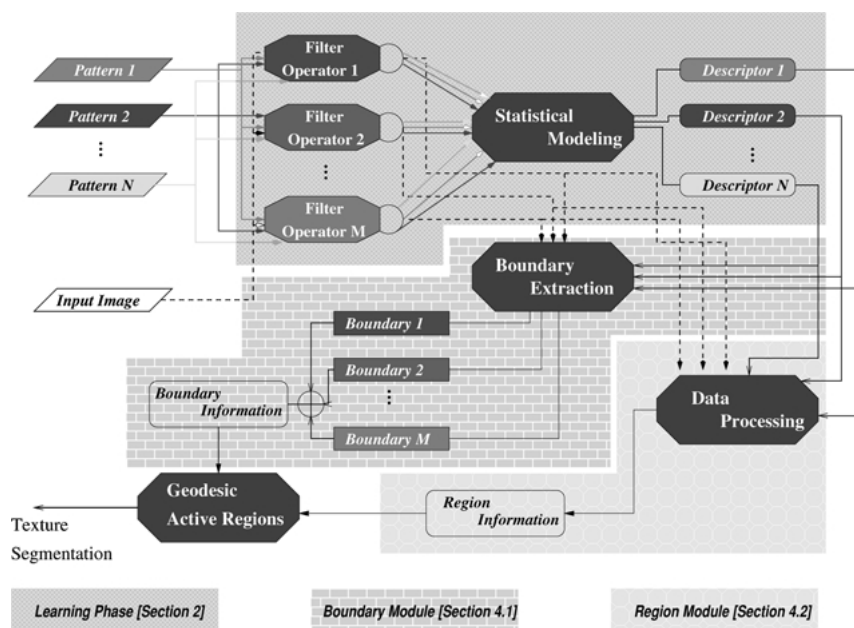


Figure 2. Geodesic Active Regions for supervised texture segmentation: The overview of the proposed framework.

segmentation map that separates the background from the other textured regions.

The proposed algorithm is depicted in Fig. 2. Initially, an off-line step is performed that creates multi-component probabilistic texture descriptors for the given set of texture patterns, where the multidimensional feature data is derived using a set of filter operators (Fig. 2: *Learning Phase*). This phase is decomposed into three steps. First, the texture features are captured using a predefined set of filter operators (Isotropic, Anisotropic and Gabor). Second, these features are modeled for each texture pattern using continuous probability density functions. The last step consists of validating these features, and refers to the estimation of some reliability measurements for the different filters operators that have been used to obtain them.

Then, given the input frame, we apply the same operators and derive an observation set that refers to the same multidimensional feature space that has been used to construct the texture descriptors. Then, for each pixel we estimate the probability of being on the boundaries between two different texture regions. Since we deal with multidimensional feature data, a probability vector is obtained. The components of this vector (e.g. boundary probabilities) are qualitative combined to a single frame to provide the *boundary-based* texture in-

formation (Fig. 2: *Boundary Module*). Besides, using the texture descriptors and the observation set we determine the *region-based* information that is derived from the most probable temporal texture assignment (Fig. 2: *Region Module*).

Then, the segmentation step is performed using a unified model that integrates a boundary and a region-based module and refers to the optimization of a curve-based objective function. The problem is stated under an improved Geodesic Active Contour model that aims at finding the best minimal length geodesic curve that consists of image pixels with high boundary probabilities, and creates regions that refer to an “optimal” grouping according to the image characteristics. We call this model *Geodesic Active Region*, since boundary and region information are cooperating in a coupled active contour model. The defined objective function is minimized using a gradient-descent method where a level set approach (Osher and Sethian, 1988) is used to implement the obtained PDE. To summarize, the resulting PDE propagates an initial contour (single or multiple seeds) towards the final segmentation map under the influence of boundary and regional/statistical forces while being constrained by internal forces (regularity).

The remainder of this paper is organized as follows. Section 2 deals with the texture analysis and modeling

problem while in Section 3, we introduce the main contribution of this paper, the *Geodesic Active Regions* model which is applied to the supervised texture segmentation problem in Section 4. Finally, experimental results and discussion appear in Section 5.

## 2. Texture Analysis and Modeling

The first step of supervised texture segmentation refers to a texture analysis and modeling phase where the goal is to create texture models/descriptors for a given set of texture patterns. During the last three decades a large number of approaches has been proposed.

Early approaches to texture modeling have made use of  $k$ -th order statistics, where tuples of  $k$  pixels are used to determine the behavior of the texture patterns. Although these methods have been widely used, they suffer from being computationally expensive (in terms of memory).

A more flexible model relies on the multi-channel filtering theory, where the retinal image is decomposed into a set of sub-bands, which are the convolution output with a given set of filters. These models have been widely considered to describe textures due to their impressive performance to texture segmentation and classification.

The last area of approaches rely on statistical modeling, where the observed texture pattern is assumed to be a probability distribution on a Random Field. These approaches are very powerful, they involve a small number of parameters but they are computationally expensive. The problem of creating powerful probabilistic texture models was analyzed extensively with a very elegant way in Greenspan et al. (1994), Wu et al. (1999), Zhu (1996) and Zhu et al. (1998).

### 2.1. Extracting Features

One of the crucial aspects of texture analysis/modeling is the extraction of proper and representative textural features and properties that are going to be used as input to the modeling phase. The importance of this step is quite evident, due to the fact that the ability of selecting the most representative features is strongly related with the performance and the discrimination power of the texture description model.

The use of filter and morphological operators has been applied successfully to a variety of computer vision applications, like edge-detection, image restora-

tion, image segmentation, texture segmentation, etc. In such a case, a set of linear and non-linear operators is applied to the input image, that creates a multidimensional feature vector (filter responses). These operators are optimally selected if each filter response refers to different textural properties, while the entire set of responses is a representative multidimensional feature space that can be easily differentiated from analogous spaces of other texture patterns. Although there is a lot of related work on the optimal filter selection for texture segmentation (Bovik et al., 1990; Dunn and Higgins, 1995), we adopt a rather large and general filter bank that is composed of isotropic and anisotropic filters:

- The Gaussian operator  $\{g(|\sigma)\}$

$$\left[ g(x, y | \sigma) = \frac{1}{\sqrt{2\pi}\sigma} e^{-\frac{x^2+y^2}{2\sigma^2}} \right]$$

- The isotropic center-surround operator (Laplacian of Gaussian)  $\{l(|\sigma)\}$ ,

$$\left[ l(x, y | \sigma) = S \left( 1 - \frac{x^2 + y^2}{2\sigma^2} \right) e^{-\frac{x^2+y^2}{2\sigma^2}} \right]$$

where  $S$  is a constant scale factor. Besides, the  $(x, y)$  anisotropic directional derivatives operators are also considered.

- The 2D Gabor operators analyze the image simultaneously in both space  $[\sigma]$ , and frequency domains  $[\theta, \phi]$ .

$$\left[ g_G(x, y | \sigma, \theta, \phi) = \frac{1}{2\pi\sigma^2} e^{-\frac{x^2+y^2}{2\sigma^2}} e^{-j2\pi(\theta x + \phi y)} \right]$$

These Gabor functions can be decomposed into two components; the real part  $[g_R(x, y | \sigma, \theta, \phi)]$  and the imaginary part  $[g_I(x, y | \sigma, \theta, \phi)]$ . The texture features are captured by the spectrum analyzer  $\{s(|\sigma, \theta, \phi)\}$  of the Gabor components,

$$s(x, y | \sigma, \theta, \phi) = \sqrt{(g_R * I)(x, y)^2 + (g_I * I)(x, y)^2}$$

smoothed by a Gaussian function, where  $(G_R * I)$  denotes the convolution operation between the image  $I$  and the filter  $G_R$ .

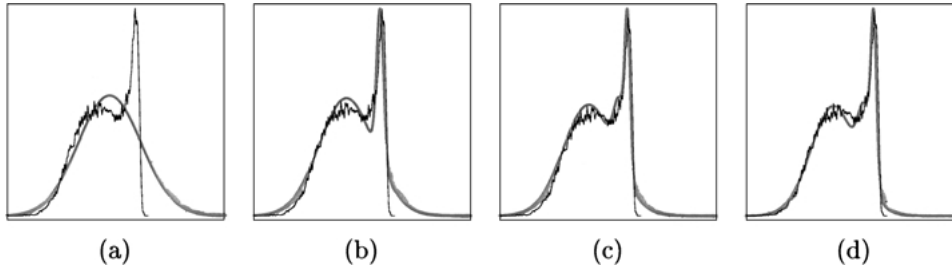


Figure 3. Mixture analysis for the zebra pattern convolution output with  $s(\cdot | 1, \pi/3, 2\pi)$  solid line: *Samples*, dashed line: *Probability density functions*. (a) one component, *mean approximation error*:  $9.76932e-05$ , *maximal*:  $0.006372$ , (b) two components, *mean approximation error*:  $3.8765e-05$ , *maximal*:  $0.003869$ , (c) three components, *mean approximation error*:  $3.4061e-05$ , *maximal*:  $0.003180$ , (d) four components, *mean approximation error*:  $3.3245e-05$ , *maximal*:  $0.002932$ .

## 2.2. Modeling Features

The modeling phase aims at finding an appropriate model that can be determined by a limited set of parameters and preserves strong discrimination power. The most common model related with filtering theory is the use of histograms. Although this model can be implemented quite easily, it encounters some important limitations. The selection of the size, as well as the number of the histogram cells affects significantly the model. These problems are more visible when the output data is not distributed uniformly. Additionally, a large number of parameters is required (histogram size) to obtain an accurate representation model. In order to deal with these problems, we adopt a statistical framework where the different filter responses are modeled using probabilities density functions that are mixture distributions of Gaussian components.

In order to facilitate the notation, let us now make some definitions:

- Let  $T = \{t_i : i \in [1, N]\}$  be the set of texture patterns.
- Let  $F = \{f_i : i \in [1, M]\}$  be the preselected set of filter operators.
- Let  $P = \{P_i : i \in [1, N]\}$  be the the set of texture pattern images and let  $D = \{D_{\{i,j\}} : i \in [1, N], j \in [1, M]\}$  be the multidimensional feature training data space, where  $D_{\{i,j\}}$  is the response of the operator  $f_j$  to the input pattern  $P_i$ .

We assume that each component [filter response] of the multidimensional feature space can be modeled using low-level statistics. Under this assumption, the statistical behavior of the data components is expressed with conditional probability density functions. Let  $p_{\{i,j\}}(\cdot)$  be the conditional probability density of

the data component  $D_{\{i,j\}}$  (normalized histogram). We assume that this probability density function is homogeneous (i.e. independent of the pixel location) and that it can be decomposed into many different components, where each component is Gaussian.

Let  $P_{\{i,j\}}^k$  be the a priori probability of the component  $k$ . The observed data values  $D_{\{i,j\}}$  are assumed to be obtained by selecting a component  $k$  with probability  $P_{\{i,j\}}^k$ , and then selecting a value  $x$  according to the probability law  $p_{\{i,j\}}^k(x | \mu_{\{i,j\}}^k, \sigma_{\{i,j\}}^k)$ . Thus, the probability density function is given by

$$p_{\{i,j\}}(x | \Theta_{\{i,j\}}) = \sum_{k=1}^{C_N} P_{\{i,j\}}^k p_{\{i,j\}}^k(x | \mu_{\{i,j\}}^k, \sigma_{\{i,j\}}^k), \quad (1)$$

where  $C_N$  is the number of mixture components, and  $\Theta_{\{i,j\}}$  is the vector of the unknown mixture parameters:  $\Theta_{\{i,j\}} = \{P_{\{i,j\}}^k, \mu_{\{i,j\}}^k, \sigma_{\{i,j\}}^k : k \in [1, \dots, C_N]\}$ . Under this hypothesis, there are two key problems: the number of different components  $C_N$ , and the estimation of the unknown parameters  $\Theta_{ij}$  of these components. In most of the cases, it has been experimentally found that two components are enough, but there are some cases where at least three/four components must be assumed. This case appears very often for texture patterns that are not homogeneous. The determination of the component number is based on the mean approximation error between the samples and the estimated mixture model. We increment the number of components until the mean approximation error drops below a given threshold. To deal with cases where this threshold cannot be satisfied, we also consider the relative improvement of the approximation when a new component is added. Concerning the example of Fig. 3, the improvement of the approximation between the use of

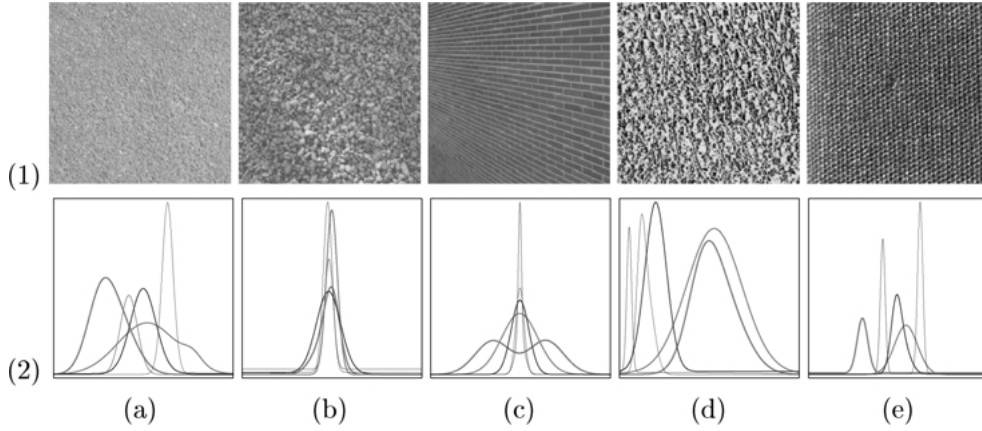


Figure 4. (1) Texture patterns, (2) statistical modeling for the operator responses. (2.a)  $g(\dots | 1)$ , (2.b)  $l(\dots | 1)$ , (2.c)  $g_R(\dots | 1, \pi/3, \pi/2)$ , (2.d)  $s(\dots | 1, \pi/3, \pi/2)$ , (2.e)  $(\dots | 1, 2\pi, 2\pi)$ . Each graph corresponds to a filter operator and contains the statistical modeling result for all texture patterns. Each color among the different graphs refers to the same texture pattern.

two and three components is not significant, thus we approximate this filter response with two components. The estimation of the unknown parameters  $\Theta_{ij}$  can be done using the maximum likelihood principle (Duda and Hart, 1973).

The output of this operation is a powerful texture description model that can be expressed using a limited set of parameters under a statistical framework. Each texture pattern is associated with a tuple of conditional probability density functions

$$\mathbf{p}_i = (p_{i,1}, \dots, p_{i,M}) : i \in [1, N]$$

that characterizes the behavior of this pattern with respect to the different filter operators (Fig. 4).

### 2.3. Validating Features

One of the pre-occupations of statistical analysis is to decrease the number of required parameters that are involved to a statistical decision problem or to validate them by assigning some reliability measurements. Using a small number of parameters, we can predict and analyze easier the behavior of the model. Furthermore, the validation of these parameters, results to a better solution since they may be considered according to their “quality”.

In our case, these parameters refer to the number of filters. The filters have different orientation and scale, reflecting in different “quality” with respect to their ability of capturing the texture features. Moreover, given a set of texture patterns, some of the filter oper-

ators are more qualified to be used, due to the fact that they better capture the observed texture properties, resulting on an observation set where the discrimination between the different textures can be easily performed. Thus, in this sub-section the validation of the different filter operators will be considered.

After the completion of this extraction and modeling phase, a tuple of probability density functions is associated with each texture pattern (the components of this tuple refer to the different filter operators). These tuples are composed of continuous density functions that measure the probability that a given value comes from the texture pattern, given the origin of the considered tuple.

Thus, given a filter operator  $[f_o]$ , a texture pattern  $[t_p]$  and the corresponding texture descriptor  $[\mathbf{p}_p]$ , we can estimate the misclassification error for this operator during the modeling phase. By considering the convolved pattern image  $[D_{\{t_p, f_o\}}]$  (the convolution result between the pattern and the operator) we can estimate the number of pixels that are misclassified. A pixel  $s$  is misclassified, *if and only if* there is another texture pattern  $[t_x]$ , for which the conditional probability given the observed value at  $s$   $[p_{\{t_x, f_o\}}(D_{\{t_p, f_o\}}(s))]$  is superior to the one that refers to the true case  $[p_{\{t_p, f_o\}}(D_{\{t_p, f_o\}}(s))]$ . Hence, for a given filter  $[f_o]$  operator and for a given texture pattern  $[t_p]$  we can estimate the number of the properly classified pixels as follows

$$P_{f_o}(t_p) = \frac{1}{|D|} \int_D \int_{\{t_p, f_o\}} \underbrace{H_{\{t_p, f_o\}}(D_{\{t_p, f_o\}}(x, y))}_{\text{Correctness function}} dx dy \quad (2)$$

where  $|D|$  is the number of grid pixels, and the function  $H_{\{t_p, f_o\}}(\cdot)$  is given by

$$H_{\{t_p, f_o\}}(a) = \underbrace{\prod_{i=1, i \neq t_p}^N [p_{\{t_p, f_o\}}(a) \geq p_{\{i, f_o\}}(a)]}_{a \text{ comes from image } D_{\{t_p, f_o\}}} \quad (3)$$

This is a binary function, which:

- is equal to *one* if the given pixel is classified correctly (the probability with respect to the true nature is superior to the other probabilities),

$$\left[ \bigcap_{i=1, i \neq t_p}^N [p_{\{t_p, f_o\}}(a) \geq p_{\{i, f_o\}}(a)] \right] = 1$$

- equal to *zero* if there is an alternative texture hypothesis that is more probable given the observed value (*the pixel is misclassified*).

$$[\exists i \in [1, N] : i \neq t_p, \quad p_{\{t_p, f_o\}}(a) < p_{\{i, f_o\}}(a)]$$

In other words, the function  $P_{f_o}(t_p)$  measures the properly classified pixels on the image  $D_{\{t_p, f_o\}}$ , and can be used as reliability measurement for the corresponding filter operator. However, during the learning phase this measurement is available  $N$  times (the number of texture patterns). This is due to the fact that a given operator is applied to the whole set of texture patterns. Hence we have to combine these reliability measurements that refer to the same filter operator into one value. This can be done very easily by averaging them (a filter operator is good if it preserves strong discrimination power for all texture patterns), hence the reliability of a given filter operator  $f_o$  is given by

$$w_{f_o} = \frac{1}{N} \sum_{i=1}^N P_{f_o}(t_i) \quad (4)$$

Moreover, these reliability measurements might be normalized as  $[\hat{w}_{f_o} = \frac{w_{f_o}}{\sum_{i=1}^M w_{f_i}}]$  for all filter operators.

### 3. Geodesic Active Regions

In order to facilitate the presentation of the most closely related boundary/region frame partition approaches and the introduction of the new model, the bi-modal case will be considered.

#### 3.1. Notation

Let us make some definitions as well as some assumptions regarding the a priori knowledge that are going to be used to present the existing frameworks and to introduce the Geodesic Active Regions model,

- Let  $I$  be the input image composed of two classes  $(h_A, h_B)$ ,
- Let  $\mathcal{P}(\mathcal{R}) = \{\mathcal{R}_A, \mathcal{R}_B\}$  be a partition of the image domain into two non-overlapping regions (Fig. 5(a)),
- Let  $\partial\mathcal{P}(\mathcal{R})$  be the boundaries between the regions  $\mathcal{R}_A$  and  $\mathcal{R}_B$  of the  $\mathcal{P}(\mathcal{R})$  partition.
- Let us make the assumption that some knowledge regarding the expected positions of real region boundaries is available, the boundary probabilities  $p_C(\cdot)$ , (the  $b$  stands for boundary) which measure the likelihood of a given pixel being at the real boundaries between the two classes  $(h_A, h_B)$  (Fig. 5(b)),
- Finally, let us also make the assumption that some knowledge regarding the expected region properties of the classes  $h_A, h_B$  is available, the region probabilities  $p_A(\cdot), p_B(\cdot)$  which measure the likelihood of a given pixel preserving the expected region properties of the considered classes  $(h_A, h_B)$  (Fig. 5(c) and (d)).

#### 3.2. Related Work

Caselles et al. (1995, 1997) and Kichenassamy et al. (1995) have proposed the *geodesic active contour* model for image segmentation as a geometric alternative for snakes which may be considered as an “extension” of the classic snake since it overcomes some of the snake limitations. A similar model that is geometry-based was proposed in Malladi et al. (1995).

Thus, according to the geodesic active contour, the desirable frame partition is obtained by minimizing (after the necessary modifications to meet the notation frame-work)

$$E(\partial\mathcal{R}) = \int_0^1 g \left( \underbrace{p_b(I(\partial\mathcal{R}_A(c)))}_{\text{boundary probability}} \right) \underbrace{|\partial\dot{\mathcal{R}}_A(c)|}_{\text{regularity}} dc \quad (5)$$

*boundary attraction*

where  $\partial\mathcal{R}(c)$  is a parameterization of the  $\mathcal{R}_A$  region boundaries into a planar form [we have implicitly the assumption that  $\mathcal{R}_A$  is the interior curve region],  $g(\cdot)$  is a

monotonically decreasing function (e.g. Gaussian) and the dot operator  $\{\partial\mathcal{R}(c)\}$  denotes the partial derivative with respect to the curve parameter  $[\partial\mathcal{R}(c) = \frac{\partial[\partial\mathcal{R}]}{\partial c}(c)]$ . The interpretation of this functional is clear since the optimal frame partition is obtained by finding the minimal length geodesic curves that are attracted by the real region boundaries. Moreover, the same authors have proposed the implementation of the obtained motion equation using the level set methods resulting on a paradigm that can deal automatically with topological changes. Summarizing, the geodesic active contour is an elaborated method for boundary-based image partition applications that is favorably compared with the classical snake model.

However, this model also encounters several limitations: (i) It only makes use of very local information (like the snake model) and is very sensitive to local minima, (ii) Due to the fact that the geodesic active contour framework relies on a non-parameterized curve, and evolves mainly an initial curve towards one direction (constrained by the curvature effect), it demands a *specific* initialization step, where the initial curve should be completely exterior or interior to the real object boundaries.

Many efforts have been made to overcome these shortcomings by introducing some region-based features to snake-based partition methods with objective to make them free from the initial conditions and more robust. Towards this direction, bi-directional boundary-based flows have been also proposed recently (Xu and Prince, 1997; Paragios et al., 2001).

Chakraborty et al. (1996) proposed a model for medical image segmentation that integrates edge and region-based information within a deformable boundary finding framework. Their objective function (after the necessary modifications to meet the notation framework) is given by

$$\begin{aligned}
 E(\partial\mathcal{R}, I_G, I_R) = & \alpha E_{PRIOR}(\partial\mathcal{R}) \\
 & + \beta \underbrace{\int_0^1 I_G(\partial\mathcal{R}(f)) df}_{\text{Boundary Term}} \\
 & + \gamma \underbrace{\int_{\mathcal{R}} \int_A I_R(x, y) dx dy}_{\text{Region Term}} \quad (6)
 \end{aligned}$$

where  $I_G$  is an image that contains the gradient norm values,  $I_R$  is an image that accounts for the region information, and  $\{\partial\mathcal{R}(f)\}$  is a parameterization of the

boundaries using Fourier descriptors. As far the interpretation of the energy components, the prior term  $E_{PRIOR}()$  introduces some prior knowledge about the shape form (the final contour should be close to this shape), the boundary term propagates the curve towards high gradient values points (edges), and the region term incorporates some region-based information into the boundary finding framework. This information is the output of a region segmentation step.

Within this framework, the boundaries are parameterized using Fourier descriptors, which present some important limitations with respect to the shapes that they can describe. Additionally, the region information is expressed *via intensity homogeneity which limits the model applicability*, even if it is not a strong constraint. Moreover, due the Lagrangian implementation of the curve propagation, the topological changes cannot be handled. Furthermore, this approach requires a pre-segmentation map  $[I_R]$ . Finally, some of the probabilistic assumptions that have been done to determine the model may be not valid if the current boundary is far away from the true boundary. Thus, the model is sensitive to the *initial conditions*. However, this is the first effort that combines successfully boundary and region-based information within a snake minimization framework.

Zhu and Yuille (1996) proposed a statistical variational approach for image/texture segmentation which combines the geometrical features of a snake/balloon model and the statistical techniques of region growing. Their objective function (after the necessary modifications to meet the notation framework) is given by

$$\begin{aligned}
 E(\partial\mathcal{R}) = & \frac{\alpha}{2} \int_0^1 |\partial\dot{\mathcal{R}}(c)| dc \\
 & + \beta \sum_{X \in \{A, B\}} \left\{ \int_{\mathcal{R}} \int_X \log(p_X(I(x, y))) dx dy \right\} \quad (7)
 \end{aligned}$$

where  $[\partial\mathcal{R}_A = \partial\mathcal{R}_B = \partial\mathcal{R}]$  (the orientation is not considered). In this approach, although a snake/balloon model is employed for the segmentation process, *the boundary-based information is ignored* and the snake/balloon model is used only to impose a regularity constraint. Besides, due to the implementation of the curve propagation using a Lagrangian approach, the changes of topology cannot be naturally handled. However, this approach can deal with the merging topological change by introducing a region growing step. Hence, regions (curves) that have common boundaries

are merged if the entropy of the resulting region is inferior to the sum of the regions entropies before merging. In any case, this step can be performed only to region growing approaches and cannot deal with the “splitting” topology change.

In parallel with the framework proposed in this paper, related variational approaches have also been introduced (Amadiou et al., 1999; Chan and Vese, 1999; Samson et al., 1999; Yezzi et al., 1999). In Chan and Vese (1999) and Samson et al. (1999) two different variational frameworks are proposed based on Mumford and Shah (1985) for bi-modal and supervised segmentation while in Yezzi et al. (1999) a three-modal approach is proposed. The Chan and Vese (1999) framework as well as the Samson et al. (1999) can be viewed as extensions of the Mumford and Shah (1985) approach where a level set implementation is considered, while the Yezzi et al. (1999) approach is inspired by the mathematical formulation proposed in Zhu and Yuille (1996). However, these frameworks do not make use of boundary-based information and are sensitive to the initial conditions since statistics are generated and update over regions dynamically. Furthermore, they are constrained (with the exception of Samson et al., 1999 where the supervised image segmentation case is considered) to bi-modal and three-modal image segmentation cases. A closely related approach to Chan and Vese (1999) was proposed in parallel in Amadiou et al. (1999). Finally, more recent approaches related with the proposed framework can be found in Tsai et al. (2000) and Chan and Vese (2001).

The Geodesic Active Regions model has been initially introduced in Paragios and Deriche (1999b) for supervised texture segmentation and then extended to deal with the un-supervised image segmentation case in Paragios and Deriche (2000a), and successfully exploited in Paragios and Deriche (1999c) to provide an elegant solution to the motion estimation and the tracking problem.

Within this framework the region boundaries are accurately extracted (opposite to Zhu and Yuille, 1996; Chan and Vese, 1999; Yezzi et al., 1999 where there is no boundary attraction) that is an important issue for many applications (e.g. segmentation of medical images). Furthermore, the proposed approach can deal automatically with topological changes (opposite to Chakraborty et al., 1996; Zhu and Yuille, 1996) where only the “merging” topology change could be handled separately to the segmentation phase through a region-growing step, is free from the initial conditions opposite to (Caselles et al., 1995; Chakraborty et al., 1996; Zhu and Yuille, 1996) where the statistics of each region are generated and updated automatically and hence the initial regions positions affect significantly the segmentation result). Finally, the Geodesic Active Regions Model does not require any pre-segmentation input (opposite to Chakraborty et al., 1996). On the other hand, the proposed segmentation framework refers to a supervised case (opposite to Zhu and Yuille, 1996; Chan and Vese, 1999; Yezzi et al., 1999 where the un-supervised case is considered).

### 3.3. Setting the Boundary Module

Thus, according to this framework, the frame partition task can be viewed initially as the problem of accurately extracting the boundaries between the regions  $\mathcal{R}_A$  and  $\mathcal{R}_B$ . This, can be done by the geodesic active contour model, thus minimizing

$$E(\partial\mathcal{R}) = \int_0^1 g \left( \underbrace{p_C(I(\partial\mathcal{R}_A(c)))}_{\text{boundary probability}} \right) \underbrace{|\partial\mathcal{R}_A(c)|}_{\text{regularity}} dc \quad (8)$$

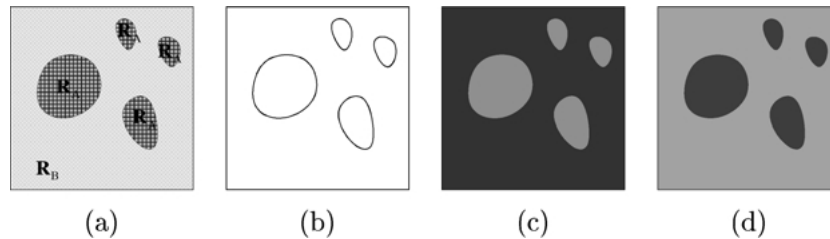


Figure 5. Geodesic Active Regions model: (a) the input, (b) the boundary-based information, (c) the region-based information corresponding to hypothesis  $h_A$ , [the information is proportional to the frame intensities] (d) the region-based information corresponding to hypothesis  $h_B$  [the information is proportional to the frame intensities].

### 3.4. Setting the Region Module

At the same time, the examined problem is equivalent to creating a consistent frame partition between the observed data, the associated hypothesis and their expected properties. This partition can be viewed as an optimization problem with respect to the a posteriori frame partition probability, given the observation set.

Let  $[p_S(\mathcal{P}(\mathcal{R}) | I)]$  be the a posteriori frame partition density function with respect to the different partitions  $\mathcal{P}(\mathcal{R})$  given the input image  $I$ . This density function is given by the Bayes rule as:

$$p_S(\mathcal{P}(\mathcal{R}) | I) = \frac{p(I | \mathcal{P}(\mathcal{R}))}{p(I)} p(\mathcal{P}(\mathcal{R})) \quad (9)$$

where

- $p(I | \mathcal{P}(\mathcal{R}))$  is the a posteriori segmentation probability for the image  $I$ , given the partition  $\mathcal{P}(\mathcal{R})$ ,
- $p(\mathcal{P}(\mathcal{R}))$  is the probability of the partition  $\mathcal{P}(\mathcal{R})$  among the space of all possible partitions of the image domain,
- and  $p(I)$  is the probability of having as input the image  $I$  among the space of all possible images.

If we assume that all the partitions are a priori equally probable  $[p(\mathcal{P}(\mathcal{R})) = \frac{1}{Z}]$  where  $Z$  is the number of possible partitions, then we can ignore the constant terms  $p(I)$ ,  $p(\mathcal{P}(\mathcal{R}))$  and the density function is equivalent with:

$$\hat{p}_S(\mathcal{P}(\mathcal{R}) | I) = p(I | \{\mathcal{R}_A, \mathcal{R}_B\}) \quad (10)$$

Besides, since normally there is no correlation between the regions labeling, and the region probabilities depend only on their observation set (within the region), we obtain the following form

$$\begin{aligned} \hat{p}_S(\mathcal{P}(\mathcal{R}) | I) &= p([I | \mathcal{R}_A] \cap [I | \mathcal{R}_B]) \\ &= p(I | \mathcal{R}_A) p(I | \mathcal{R}_B) \end{aligned} \quad (11)$$

where  $p(I | \mathcal{R}_A)$  is the a posterior probability for the region  $\mathcal{R}_A$  given the corresponding image intensities (resp.  $p(I | \mathcal{R}_B)$ ).

Finally, if we assume that the pixels within each region are independent that is a commonly used assumption, then we can replace the region probability by the

joint probability among the region pixels:

$$p(I | \mathcal{R}_X) = \prod_{s \in \mathcal{R}_X} p_X(I(s)) \quad (12)$$

where  $X \in \{A, B\}$ .

Taking all these into account, the a posteriori segmentation probability for a partition  $\mathcal{P}(\mathcal{R})$  given the observed image  $I$  is determined by

$$\hat{p}_S(\mathcal{P}(\mathcal{R}) | I) = \prod_{s \in \mathcal{R}_A} p_A(I(s)) \prod_{s \in \mathcal{R}_B} p_B(I(s)) \quad (13)$$

The maximization of the simplified a posteriori segmentation probability is equivalent to the minimization of the  $[-\log(\cdot)]$  function of this probability,

$$\begin{aligned} E(\partial \mathcal{P}(\mathcal{R})) &= \underbrace{\int_{\mathcal{R}_A} \int \log \left[ \underbrace{p_A(I(x, y))}_{h_A \text{ probability}} \right] dx dy}_{\mathcal{R}_A \text{ fitting measurement}} \\ &\quad - \underbrace{\int_{\mathcal{R}_B} \int \log \left[ \underbrace{p_B(I(x, y))}_{h_B \text{ probability}} \right] dx dy}_{\mathcal{R}_B \text{ fitting measurement}} \end{aligned} \quad (14)$$

This term is similar with the one proposed in Zhu and Yuille (1996).

Let us now try to interpret this region-based term:

- Suppose that a pixel  $s$  is well classified and the true case is  $h_A$ ; then this pixel appears to the  $\mathcal{R}_A$  fitting measurement. The corresponding probability for the true case  $[p_A(I(s))]$  is higher than the one for the opposite case  $[p_B(I(s))]$ , resulting on a minimum contribution in the objective function  $[-\log(p_A(I(s)))]$ .
- On the other hand if this pixel is not appropriately classified, then it appears for example to the  $\mathcal{R}_A$  fitting measurement while the true case is  $h_B$ . It is obvious to see that the penalization of the objective function due to the mis-labeling of this pixel will be higher compared by the one introduced if the appropriate decision was taken.

Summarizing, this region-based energy term is defined using the partition determined by the curve and aims at maximizing the a posteriori segmentation probability given the input image.

### 3.5. Geodesic Active Regions Objective Function

Then, the two different frame partition modules are integrated by defining the Geodesic Active Regions objective function as

$$\begin{aligned}
 E(\partial\mathcal{R}) = & \alpha \int_0^1 g \left( \underbrace{p_C(I(\partial\mathcal{R}_A(c)))}_{\text{boundary probability}} \right) \underbrace{|\partial\dot{\mathcal{R}}_A(c)|}_{\text{regularity}} dc \\
 & - (1 - \alpha) \underbrace{\int_{\mathcal{R}_A} \int \log \left[ \underbrace{p_A(I(x, y))}_{h_A \text{ probability}} \right] dx dy}_{\mathcal{R}_A \text{ fitting measurement}} \\
 & - (1 - \alpha) \underbrace{\int_{\mathcal{R}_B} \int \log \left[ \underbrace{p_B(I(x, y))}_{h_B \text{ probability}} \right] dx dy}_{\mathcal{R}_B \text{ fitting measurement}}
 \end{aligned} \tag{15}$$

where  $\alpha$  is a positive constant that balances the contributions of the two terms [ $0 \leq \alpha \leq 1$ ].

The interpretation of the defined objective function is following.

We seek a set of curves that:

- i. [Boundary Term] are *regular* [Eq. (15): *regularity*], of minimal length, and are attracted by the real regions boundaries [Eq. (15): *boundary attraction*],
- ii. [Region Term] define a partition of the image which maximizes the a posteriori frame partition probability.

The minimization of the objective function is performed using a gradient descent method. If  $u = (x_A, y_A)$  is a point of the initial curve  $\partial\mathcal{R}_A$  and we compute the Euler-Lagrange equations using the Stokes theorem (Caselles et al., 1997; Zhu and Yuille, 1996), then we should deform the curves ( $\partial\mathcal{R}_A$ ) using the following equation:

$$\left\{ \begin{aligned}
 \frac{\partial u}{\partial t} = & \alpha \log \left( \underbrace{\frac{p_B(I(u))}{p_A(I(u))}}_{h_B \text{ probability}} \right) \mathcal{N}(u) \\
 & + \underbrace{(1 - \alpha)(g(p_C(I(u)))\mathcal{K}(u) - \nabla_g(p_C(I(u))) \cdot \mathcal{N}(u))}_{\text{Boundary-based force}}
 \end{aligned} \right. \tag{16}$$

The obtained PDE motion equation has two kind of *forces* acting on the propagating curves in the direction of the inward normal:

- *Region Force*: This force aims at shrinking or expanding the curve in the direction that maximizes the a posteriori segmentation probability. Let us now try to interpret this force for a given curve pixel  $u$  by reminding that this pixels is associated to the  $h_A$  class,
- if the true state of  $u$  is  $h_B$ , then the conditional density function that accounts for this class [ $p_B(I(u))$ ] should support the true case [ $p_B(I(u)) > p_A(I(u))$ ], resulting on a positive force that aims at shrinking the curve to pass through this pixel:

$$\begin{aligned}
 p_B(I(u)) > p_A(I(u)) & \Rightarrow \frac{p_B(I(u))}{p_A(I(u))} > 1 \\
 & \Rightarrow \log \left( \frac{p_B(I(u))}{p_A(I(u))} \right) > 0 \\
 & \Rightarrow \alpha \log \left( \frac{p_B(I(u))}{p_A(I(u))} \right) > 0
 \end{aligned}$$

- On the other hand, if the true state of  $u$  is the  $h_A$ , then this force aims at expanding the curve to include this pixel.
- The *boundary force* contains information regarding the boundaries of the different regions and is composed of two sub-terms; one that shrinks the curve constrained by the curvature effect towards the object boundaries and one that attracts the curve to the objects boundaries (refinement term).

### 3.6. Model Generalization

The main assumption that has been made to provide the proposed framework relies on the fact that all partitions are equally probable. Generally, this is assumption is not valid, but this does not constrain the proposed model since the same framework can be recovered by replacing the a posteriori frame partition probability with the *joint* probability that is a commonly used as a region-based optimization criterion.

The proposed model can be generalized very easily by assuming for a specific application the existence of functions that capture the boundary and the region properties of the different regions. Thus, if we consider

- A frame partition problem with  $N + 1$  classes [ $N$  classes plus the background class  $\mathcal{R}_0$ ],
- A set of boundary attraction functions [ $b_i : \mathcal{R} \times \mathcal{R} \rightarrow \mathcal{R}, i \in [1, N]$ ] that “capture” the boundary features of the different classes (*for the real boundary pixels this function returns minima values*),
- A set of region homogeneity functions [ $r_i : \mathcal{R} \times \mathcal{R} \rightarrow \mathcal{R}, i \in [1, N]$ ] that “capture” the region features of the different classes (*for the real class pixels this function returns minima values*),

then, the Geodesic Active Regions framework consists of minimizing:

$$\begin{aligned}
 E(\partial\mathcal{R}) = & \sum_{i=1}^N \alpha \underbrace{\int_{\mathcal{R}_i} \int r_i(I(x, y)) dx dy}_{\text{i Region Term}} \quad \mathcal{R}_i \text{ fitting measurement} \\
 & + \sum_{i=1}^N (1 - \alpha) \underbrace{\int_0^1 \underbrace{b_i(I(\partial\mathcal{R}_i(c_i)))}_{\text{i boundary attraction}} \underbrace{|\partial\mathcal{R}_i(c_i)|}_{\text{i regularity}} dc_i}_{\text{Boundary Term}}
 \end{aligned} \tag{17}$$

The minimization of the generalized objective function is performed using a gradient descent method and leads to a system of  $N$  motion equations (one for each class/curve) given by,

$$\left\{ \begin{array}{l} \forall_i \in [1, N] \\ \frac{\partial u_i}{\partial t} = \underbrace{\alpha(r_i(u_i) - r_{o_i}(u_i)) \mathcal{N}_i(u_i)}_{\text{i region force}} \\ \quad + \underbrace{(1 - \alpha)(b_i(u_i) \mathcal{K}_i(u_i) - \nabla b_i(u_i) \cdot \mathcal{N}_i(u_i)) \mathcal{N}_i(u_i)}_{\text{i boundary force}} \end{array} \right. \tag{18}$$

where the assumption that the pixel  $u_i$  lies between the regions  $\mathcal{R}_i$  and  $\mathcal{R}_{o_i}$  has been made implicitly. According to the above equations, a given curve is propagated along its normal direction under the influence of two forces:

- A region-based force that moves the curves towards the direction that creates the optimal frame partition (according to “*region properties*”) map using the the observation set and the expected properties of the different classes,
- A boundary-based force that shrinks the curve under the influence of a regularity constraint (curvature

effect) towards the different region boundaries (according to the “*boundary properties*”).

Then, the proposed framework is employed as follows: Initially a set of random curves is used to initialize the region positions. Then, each region is deformed according to the corresponding motion (Eq. (18)) towards the final frame partition. The interaction between the regions positions is obtained through the region-based force since for a given pixel that is attributed to two different regions, forces with opposite signs appear to the corresponding motion [PDE] equations.

### 3.7. Level Set Methods

The obtained motion equations can be implemented using a difference approximation scheme (Lagrangian approach). However, in that case the evolving model cannot deal with topological changes and numerical approximations can be very unstable. These limitations can be dealt with by introducing the pioneering work of Osher and Sethian (Osher and Sethian, 1988; Sethian, 1996; Osher and Fedkiw, 2000), the level set theory (Fig. 6) where the central idea is to represent the moving front  $\partial\mathcal{R}(c, t)$  as the zero-level set

$$\phi(\partial\mathcal{R}(c, t), t) = 0$$

of a function  $\phi$ . This representation of  $\partial\mathcal{R}(c, t)$  is implicit, parameter-free and intrinsic. Additionally, it is topology-free since different topologies of the zero level-set do not imply different topologies of  $\phi$ . It easy to show, that if the moving front evolves according to

$$\frac{\partial}{\partial d} \partial\mathcal{R}(c, t) = F(\partial\mathcal{R}(c, t)) \mathcal{N}$$

for a given function  $F$ , then the embedding function  $\phi$  deforms according to

$$\frac{\partial}{\partial d} \phi(p, t) = F(p) |\nabla \phi(p, t)|$$

For this level-set representation, it is proved that the solution is independent of the embedding function  $\phi$ . A common selection for the embedding function refers to the signed Euclidean distance from the evolving interface.

Thus, the system of motion equations that drives the curve propagation for the Generalized Geodesic Active

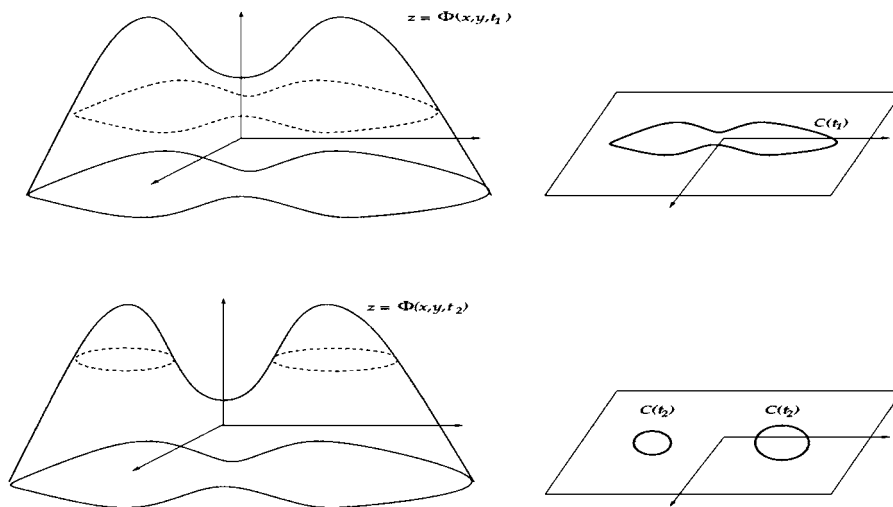


Figure 6. Level set methodology and curve propagation. The left figure column shows the evolving level set function, while on the right the curve corresponding to the zero level set values of the surface. The mechanism that allows changes of topology is also illustrated.

Regions framework is transformed into a system of multiple surfaces evolution given by,

$$\left\{ \begin{array}{l} \forall i \in [1, N] \\ \frac{\partial \phi_i}{\partial t}(u) = \underbrace{\alpha(r_i(u) - r_{o_i}(u)|\nabla \phi_i(u)|)}_{i \text{ region force}} \\ + (1 - \alpha) \underbrace{\left( b_i(u) \mathcal{K}_i(u) + \nabla b_i(u) \cdot \frac{\nabla \phi_i(u)}{|\nabla \phi_i(u)|} \right)}_{i \text{ boundary force}} |\nabla \phi_i(u)| \end{array} \right. \quad (19)$$

In order to demonstrate the proposed model, the task of image segmentation is considered for a synthetic frame that is composed of two classes (Fig. 7).

- The first  $[h_B]$  refers to the background and is composed from pixels with intensities that follow a Gaussian distribution with a mean value equal to 150 and a standard deviation equal to 10  $[p_B(\cdot) \sim G(150, 10)]$ ,
- The second  $[h_A]$  refers to a region composed of four components, and pixels with intensities that follow Gaussian distribution with a mean value equal to 90 and a standard deviation equal to 10  $[p_A(\cdot) \sim G(90, 10)]$ ,

For this case, the boundary information is determined using a Gaussian edge detector, applied on the norm of the gradient values space. The curve evolution

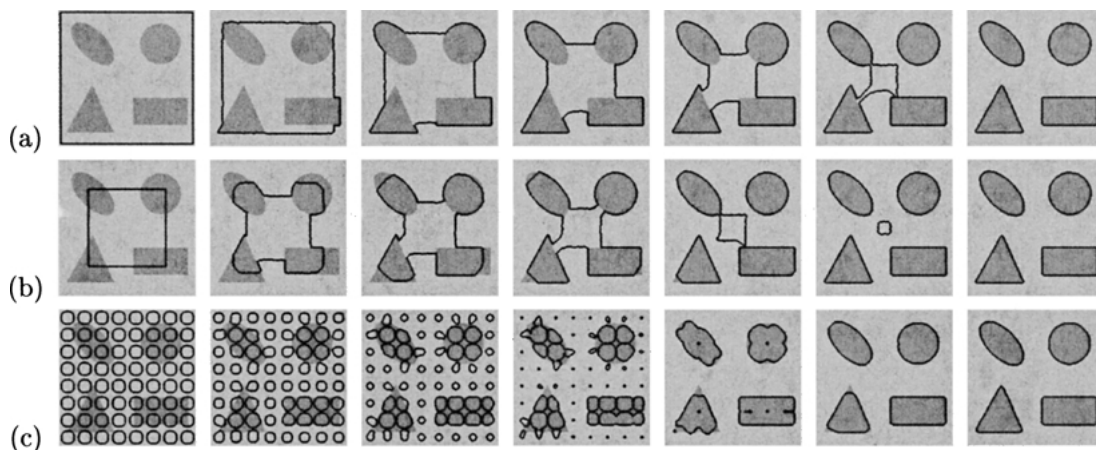


Figure 7. Geodesic Active Regions: A new paradigm to deal with frame partition problems in computer vision. The proposed framework is used for image segmentation where the independence form the initial conditions and the ability to deal with topological changes are demonstrated.

for the class  $h_A$  with respect to three different initialization steps is illustrated in Fig. 7.

#### 4. Geodesic Active Regions for Supervised Texture Segmentation

The texture segmentation problem can be viewed as a frame partition problem [defined by a curve] into non-overlapping regions that preserve *homogeneous textural properties* and *characteristics*. Some complementary definitions are required:

- Let  $I$  be the input textured frame and let  $D(I) = \{I_j : j \in [1, M]\}$  be the set of filter responses to this frame [the convolution output between the input image and the various filter operators].
- Let  $\mathcal{P}(\mathcal{R}) = \{\mathcal{R}_i : i \in [1, N]\}$  be a partition of frame domain into  $N$  non-overlapping regions,
- Let  $\partial\mathcal{P}(R) = \{\partial\mathcal{R}_i : i \in [1, N]\}$  be the region boundaries of the partition  $\mathcal{P}(R)$ .
- Let  $t_i$  be the texture pattern that is assigned to the region  $\mathcal{R}_i$ , and let  $p_{\{t_x, B\}}(s)$  be the boundary probability for a given pixel  $s$  being at the boundaries of the region  $\mathcal{R}_x$ ,

Then, the objective of the proposed framework is either to separate the background region from the other texture regions (extraction of the background region), or to extract the region of a specific texture pattern. In both cases, the unknown variable of the model refers to a curve  $\partial\mathcal{R}$  that is propagated towards the boundaries between the selected region and the other textured regions.

##### 4.1. Setting the Boundary Module

In order to properly use the Geodesic Active Region model, information regarding the real boundaries of each region has to be extracted. It is well known that the extraction of boundary information for textured images is a very tougher task.

Let  $s$  be a pixel of the image,  $N(s)$  a partition of its local neighborhood, and the  $N_R(s)$  and  $N_L(s)$  be the local subregions associated with this partition. Moreover, let  $p_{B_k}(I(N(s)))$  be the boundary probability density function with respect to the  $k$  hypothesis,  $[p(I(N(s)) | B_k)]$  be the conditional boundary probability and  $[p(I(N(s)) | \bar{B}_k)]$  be the conditional non-boundary probability. Then, using the Bayes rule and making some assumptions regarding the global a priori boundary probability (Paragios and Deriche, 1999a) it can be easily shown that the probability for a pixel  $s$  being at the boundaries of  $t_k$  texture region, given a neighborhood partition  $N(s)$  is given by,

$$p_{B_k}(s) = \frac{p(I(N(s)) | B_k)}{p(I(N(s)) | B_k) + p(I(N(s)) | \bar{B}_k)} \quad (20)$$

Then, the conditional boundary/non-boundary probabilities can be estimated directly from known quantities (see Paragios and Deriche (1999d) and Zeng et al. (1998) for details) as follows:

$k$  Boundary Condition (Fig. 8(a)):

If  $s$  is a  $t_k$  boundary pixel, then there is a partition  $[N_L(s), N_R(s)]$  where the most probable texture assignment for the “left” local region is  $t_k$  and for the “right”  $t_j$  [ $j \neq k$ ], or vice-versa,

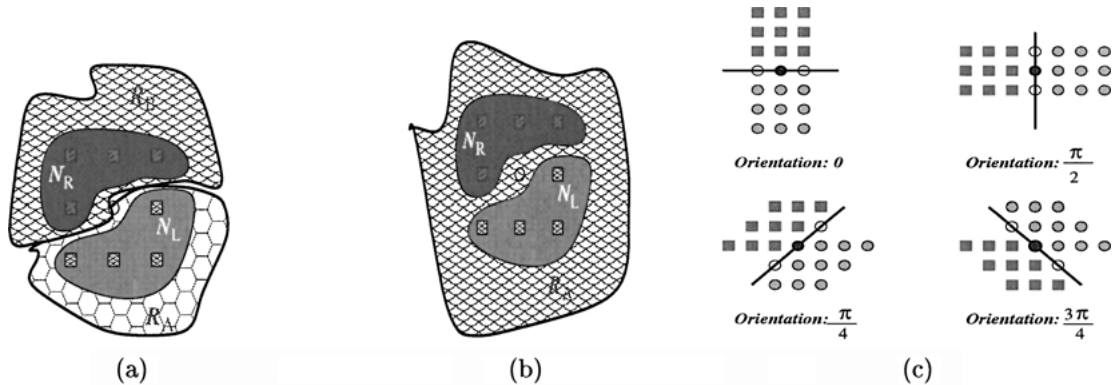


Figure 8. (a) Neighborhood partition that indicates a boundary point, (b) Neighborhood partition that indicates a non-boundary point, (c) Neighborhood partitions that are considered.

*k* Non-Boundary Condition (Fig. 8(b)):

On the other hand, if  $s$  is not a  $t_k$  boundary pixel, then for every possible neighborhood partition the most probable texture assignment for the “left” as well as for the “right” local region is  $t_k$ , or  $t_i$  and  $t_j$  where  $\{i, j\} \neq k$ .

As a consequence, the conditional  $k$  boundary/non-boundary probability density functions are given by,

$$\begin{aligned} p(I(N(s)) | B_k) &= \underbrace{p_k(I(N_R(s)))p_j(I(N_L(s)))}_{N_R(s) \in \mathcal{R}_k \cap N_L(s) \in \mathcal{R}_j} \\ &+ \underbrace{p_j(I(N_R(s)))p_k(I(N_L(s)))}_{N_R(s) \in \mathcal{R}_j \cap N_L(s) \in \mathcal{R}_k} \\ p(I(N(s)) | \bar{B}_k) &= \underbrace{p_k(I(N_R(s)))p_k(I(N_L(s)))}_{N_L(s) \in \mathcal{R}_i \cap N_R(s) \in \mathcal{R}_j} \\ &+ \underbrace{p_i(I(N_R(s)))p_j(I(N_L(s)))}_{N_L(s) \in \mathcal{R}_k \cap N_R(s) \in \mathcal{R}_k} \end{aligned} \quad (21)$$

where  $\{i, j\}$  can be identical and

- $p_k(I(N_R(s)))$  is the probability of “right” local region  $[N_R(s)]$  being part of the  $k$  region hypothesis, given the observed intensity values within this region  $[I(N_R(s))]$ ,
- $p_j(I(N_L(s)))$  is the probability of “left” local region  $[N_L(s)]$  being part of the  $j$  region hypothesis, given the observed intensity values within this region  $[I(N_L(s))]$ .

Given the definition of the probability for a pixel  $s$  being a  $k$  boundary point, the next problem is to define the neighborhood partition. We consider four different partitions of the neighborhood and the local neighborhood regions are considered to be  $3 \times 3$  directional windows (Fig. 8(c)).

Since the objective of our approach is either to distinguish the background texture region  $t_{R_0}$  from the other regions or the region that corresponds to the texture of interest (to simplify the notation we assume that this region is also the  $\mathcal{R}_0$ ), we have to estimate only the boundary probability for the  $t_{R_0}$  hypothesis. This can be done very easily since if a give pixel is a  $t_{R_0}$  boundary point then there is partition for which:

- According to the observation set, for one of the local regions the most probable texture assignment is  $t_{R_0}$ ,

- The most probable texture assignment for the other local region is different than  $t_{R_0}$ .

Hence in practice for each pixel of the image and for each partition we check whether or not the most probable hypothesis is the background one. If there is a local region with most temporal texture assignment  $t_{R_0}$ , then the boundary probability  $[p_C]$  is estimated according to the (Eq. (20)). Otherwise the boundary probability with respect to the  $t_{R_0}$  hypothesis for the given pixel is set to zero. Furthermore, if there are more than one local partitions that determines non-zero boundary probabilities, then the highest boundary probability value is considered.

This operation provides  $M$  boundary probabilities for a given pixel being at the boundaries of  $\mathcal{R}_0$ , which have to be combined into a single value. This is done using the reliability measurements that have been associated to the filter operators during the learning phase,

$$p_C(s) = \sum_{j=1}^M \hat{w}_{f_j} p_{\{C,j\}}(s) \quad (22)$$

where  $p_{\{C,j\}}(s)$  is the boundary probability of pixel  $s$  being at the boundaries of  $\mathcal{R}_0$  according to the  $I_j$  data (convolution between  $f_j$  operator and  $I$  image).

Then, the boundary-based supervised texture segmentation module can defined as follows

$$E(\mathcal{P}(\mathcal{R})) = \int_0^1 g \left( \underbrace{p_C(\partial \mathcal{R}(c))}_{\text{boundary probability}} \right) \underbrace{|\partial \mathcal{R}(c)|}_{\text{Regularity}} dc \quad (23)$$

where  $g()$  is a Gaussian function.

The efficiency of the boundary-based supervised texture segmentation module has been demonstrated in Paragios and Deriche (1999a) (the concept). The main drawback of this limited approach is that it is sensitive to the initial conditions. In other words, it demands an initial curve that includes totally the corresponding region of interest or it is included by it. Thus, cases where a region is surrounded completely by other regions cannot be dealt with by the boundary-based module. However, the obtained results were very satisfactory (Fig. 9).

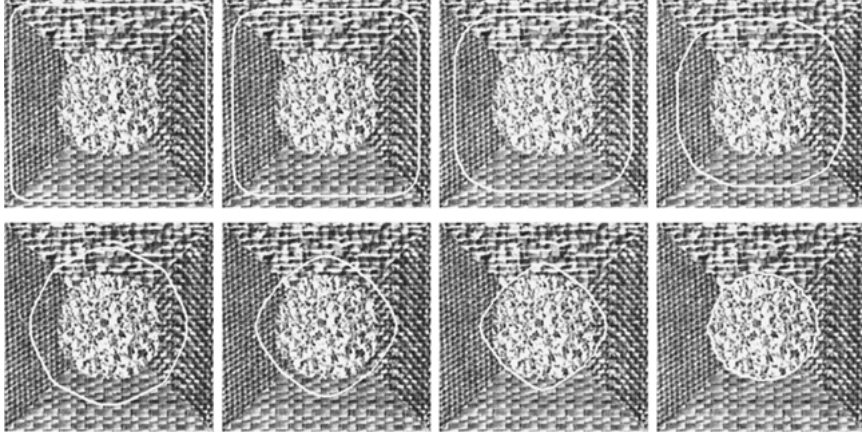


Figure 9. Geodesic Active Contours for supervised texture segmentation (Paragios and Deriche, 1999a). Demonstration for a synthetic image where the objective is to detect a specific region of interest.

#### 4.2. Setting the Region Module

Let  $p(\mathcal{P}(R) | D(R))$  be the a posteriori segmentation probability with respect to the partition  $\mathcal{P}(R)$ . Since the a posteriori region probabilities  $p(D(I)(R_i) | t_{R_i})$  are independent, the global a posteriori segmentation probability is given by,

$$\begin{aligned} p(\mathcal{P}(R) | D(I)) &= p\left(\bigcap_{i=0}^N [D(\mathcal{R}_i) | t_{R_i}]\right) \\ &= \prod_{i=0}^N p(D(\mathcal{R}_i) | t_{R_i}) \end{aligned} \quad (24)$$

where  $D(\mathcal{R}_i)$  is the multidimensional feature data associated with the region  $\mathcal{R}_i$ . Since the observation set refers to multidimensional feature data, the region/statistical term refers to multi-variate conditional probabilities. In order to simplify the model, we can assume independence between the different filter responses (since can be combined using reliability measurements) and then the a posteriori segmentation probability is given by

$$p(\mathcal{P}(R) | D(I)) = \prod_{i=0}^N \prod_{j=1}^M p(I_j(\mathcal{R}_i) | t_{R_i}) \quad (25)$$

where  $p(I_j(\mathcal{R}_i) | t_{R_i})$  is the a posterior segmentation probability for the region  $\mathcal{R}_i$  with the respect to the data component  $I_j$ .

To overcome the limitations and the errors that provokes the assumption that the different filter responses

are independent (see in DeBonet and Viola, 1998) how these dependencies can be modeled), we combine them using their reliability measurements  $w_j$ . Then, the Geodesic Active Regions functional for supervised texture segmentation consists of minimizing

$$\begin{aligned} E(\partial\mathcal{P}(\mathcal{R})) &= (1 - \alpha) \int_0^1 g \left( \underbrace{p_C(\partial\mathcal{R}(c))}_{\text{boundary probability}} \right) \underbrace{|\partial\mathcal{R}(c)|}_{\text{Regularity}} dc \\ &\quad - \alpha \underbrace{\sum_{i=0}^N \int_{\mathcal{R}_i} \int_{j=1}^M w_j \log \left[ \underbrace{p_{(t_{R_i}, j)}(I_j(x, y))}_{\text{i region probability}} \right]}_{\text{i region attraction}} dx dy \end{aligned} \quad (26)$$

The interpretation of the above function is clear and aims at finding a regular curve that is attracted by the real boundaries between the background region (or the region of interest) and the other region textures regions, while at the same time it aims at creating an image partition that maximizes the a posteriori segmentation probability.

#### 4.3. Minimizing the Objective Function

Let  $u = (x, y)$  be a point of the initial curve. This point can either be at region  $\mathcal{R}_0$  or at region  $\mathcal{R}_k$ . Based on this hypothesis, we compute the Euler-Lagrange equations (Caselles et al., 1997; Zhu and Yuille, 1996) (Section 3), and we derive the following motion equation

for  $u$ :

$$\frac{\partial u}{\partial t} = \left[ \alpha \sum_{j=1}^N w_j \log \left( \frac{P_{\{t_{R_0}, j\}}(I_j(u))}{P_{\{t_{R_k}, j\}}(I_j(u))} \right) \right. \\ \left. (1 - \alpha)(g(p_C(u))\mathcal{K}(u) - \nabla g(p_C(u)) \cdot \mathcal{N}(u)) \right] \mathcal{N}(u) \quad (27)$$

The interpretation of the above PDE is obvious. Given a initial curve, it creates a partition of the image [determined by a curve that attracts the region boundaries] where the exterior curve region corresponds to the *background* pattern (or the pattern of interest) while the interior regions correspond to the other patterns.

The obtained PDE is implemented using the level set methods where the following equation is used to update the level set function

$$\frac{\partial \phi}{\partial t}(u) = \alpha \sum_{j=1}^N w_j \log \left( \frac{P_{\{t_{R_0}, j\}}(I_j(u))}{P_{\{t_{R_k}, j\}}(I_j(u))} \right) |\nabla \phi(u)| \\ + (1 - \alpha) \left( g(p_C(u))\mathcal{K}(u) - \nabla g(p_C(u)) \cdot \frac{\nabla \phi(u)}{|\nabla \phi(u)|} \right) |\nabla \phi(u)| \quad (28)$$

In order to decrease the required computational cost of the level set implementations, we use the Narrow Method (Adalsteinsson and Sethian, 1995). The essence of this method is to perform the level set propagation only within a limited zone that is located around the latest position of the propagating contours (in the inward and outward direction). Thus, the working area is reduced significantly resulting on a significant decrease of the computational complexity per iteration. However, this method requires a frequent re-initialization of the level set functions that is performed using the Fast Marching algorithm (Sethian, 1996) is used. A similar algorithm within the area of automatic control was proposed in Tsitsiklis (1995). The re-initialization requirement can be avoided by modifying the level set embedding function as proposed in Gomes and Faugeras (2000). Although for hyper-surfaces this method will significantly decrease the computational cost, the complexity induced by this selection for 3D level set surfaces is slightly higher than the classical one.

An alternative way to further decrease the computational cost is by considering Hermes algorithm

(Paragios and Deriche, 2000b) that proposes a fast way to deform the initial curve towards the minimum of the objective function. In our case the equation which deforms the initial curve can be rewritten in a more general form as:

$$\Phi_{(x,y)}^{t+1} = \Phi_{(x,y)}^t + \mathcal{V}(x, y, \Phi) dt \quad (29)$$

where  $\mathcal{V}(x, y, \Phi)$  is the propagation speed function, depending on geometric features and image features. Since the speed  $\mathcal{V}(x, y, \Phi)$  is basically estimated according to image characteristics, there are some points for which the front evolves faster compared to the others. The key idea on which the Hermes approach is based is to evolve the front locally according to the propagation values of its points. The algorithm at each step selects the point with the highest absolute propagation speed from a set of actual curve points, and deforms the level-set image locally.

#### 4.4. Implementation Issues

The proposed method can be used to segment a given texture frame, in the case where the *background* texture pattern is known (Figs. 10 and 13). This method can be easily extend to extract some specific regions of interest determined by the corresponding *preferable* patterns (Figs. 11 and 12). In both cases, the curve propagation requires a texture assignment for the given point that has to be compared with the *preferable* assignment. This issue is confronted by assuming that the temporal segmentation map is derived by the most probable texture assignments. Thus for a given curve point, we assume that it is located between the *background or preferable* region and the region that corresponds to the most probable assignment (which is derived from the observed data). Moreover, to increase the robustness to the noise presence the region probabilities are estimated over blocks.

The proposed framework can be easily extended to *provide image segmentation* (Paragios and Deriche, 2000a). In that case, the propagation of multiple curves has to be considered where each curve remains regular, moves towards the the boundaries of a specific region and creates a region that maximizes the *joint segmentation probability* with respect to the associated hypothesis. Moreover, an interaction between these propagations can be defined that imposes the concept of mutually exclusive propagating curves.

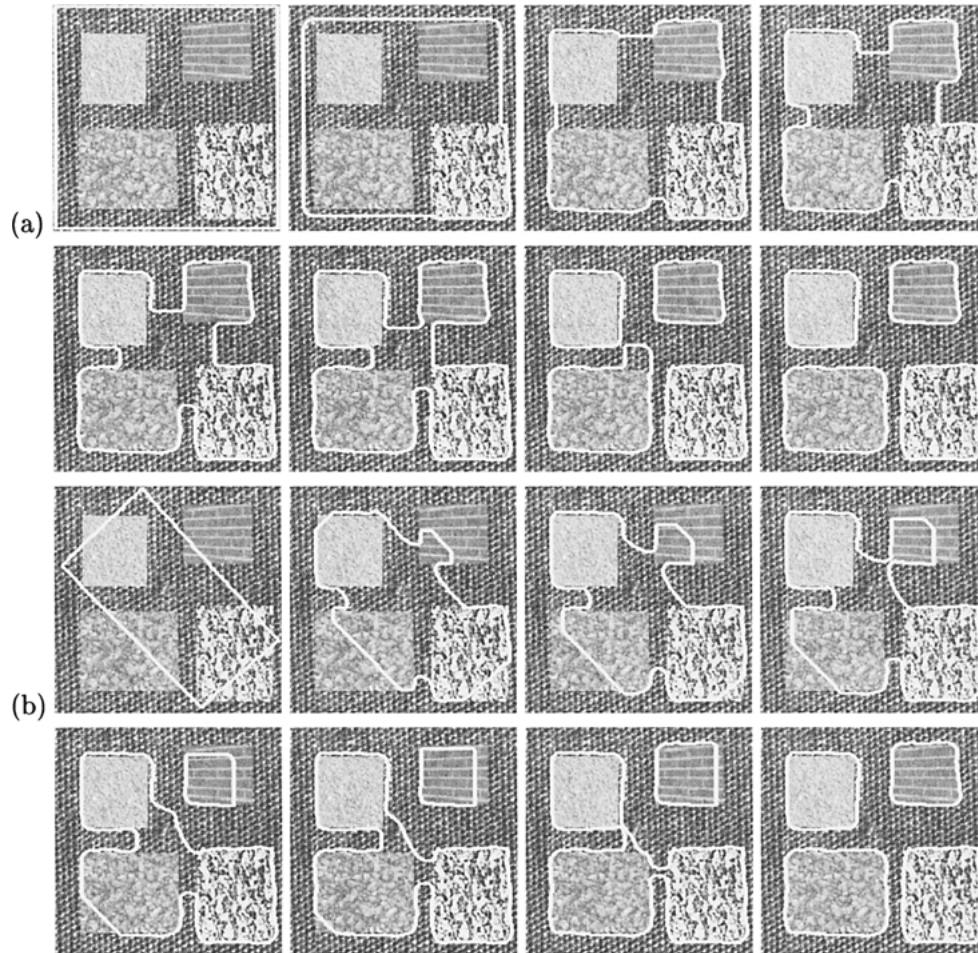


Figure 10. Geodesic Active Regions of supervised texture segmentation. The task of segmentation is considered (separation between the background texture region and the others) for a synthetic image.

## 5. Conclusions and Results

In this paper, we presented some new ideas concerning the integration of boundary-based and region-based approaches to deal with frame partition problems. The proposed framework was validated using the task of supervised texture segmentation.

### 5.1. Experimental Results

Real-world texture frame, as well synthetic texture frames have been used to test and validate the proposed approach.

Concerning the synthetic case, some texture patterns have been selected from a database of texture images. As a first step, the system is taught on these patterns by applying the bank of preselected filters and analyzing

their responses. The output of this operation is the creation of a global statistical description model for each pattern. Then, a synthetic frame is created where regions of the selected texture patterns appear randomly. This is considered as the input frame, on which the same bank of preselected filters is applied. Then, using the different filter responses, as well as the texture description models, the Geodesic Active Regions model is activated, and deforms the initial curve to the optimal solution of the texture segmentation problem.

The first experimental result shown (Fig. 10) involves a texture synthesis frame with five different texture regions, where two different contour initializations are shown. The large number of different texture regions requires the selection of a representative filter bank. In this example, the well-known level-set property of changing the topology is demonstrated,

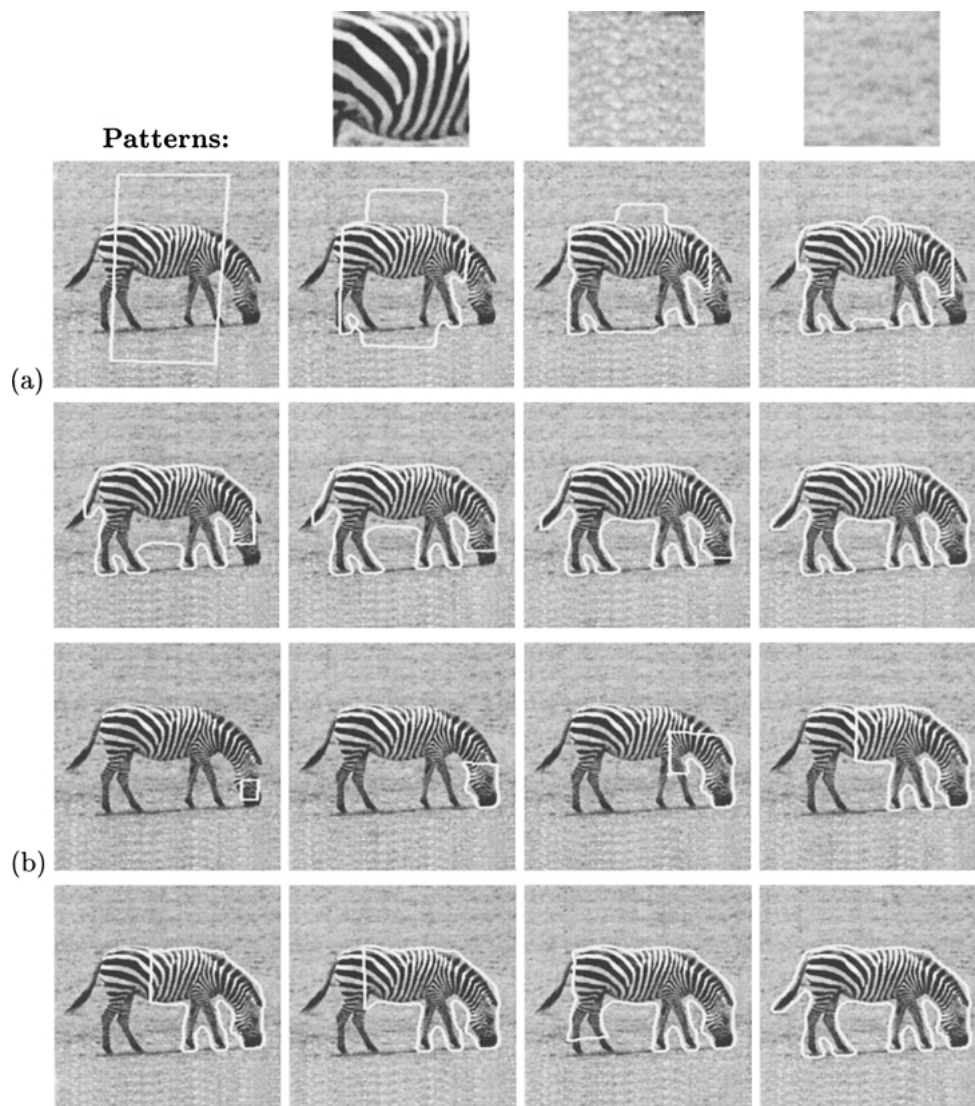


*Figure 11.* Geodesic Active Regions of supervised texture segmentation. The task of the extraction of a specific region of interest is considered for a real image (zebra).

where the initial curve breaks into multiple curves corresponding to the different texture regions.

The real case is differently treated and the inverse operation is followed (Figs. 11–13). Small patterns are selected to represent the different texture patterns appearing to this frame, and the system is taught with these patterns. Then the same process is followed as in the case of synthetic texture frames. Concerning the first “real-world” example that consists of two demonstrations (*zebra*, *chita*) (Figs. 11 and 12), we select from a  $256 \times 256$  textured frame three different window patterns  $64 \times 64$  (resp.  $96 \times 96$ ) that are the dif-

ferent texture patterns, and based on these patterns, we activate the Geodesic Active Region Models, which segments quite well the different texture regions. The independence of the model from the contour initialization is clearly demonstrated using two different contour initializations. The second “real-world” example is related to medical imagery (Fig. 13); it is a microscopic medical image of the breast, which exhibits an inflammatory carcinoma with metastasis. Three different texture patterns have been selected, and nine different filters have been applied, which give as output the texture description models. The power of the Geodesic

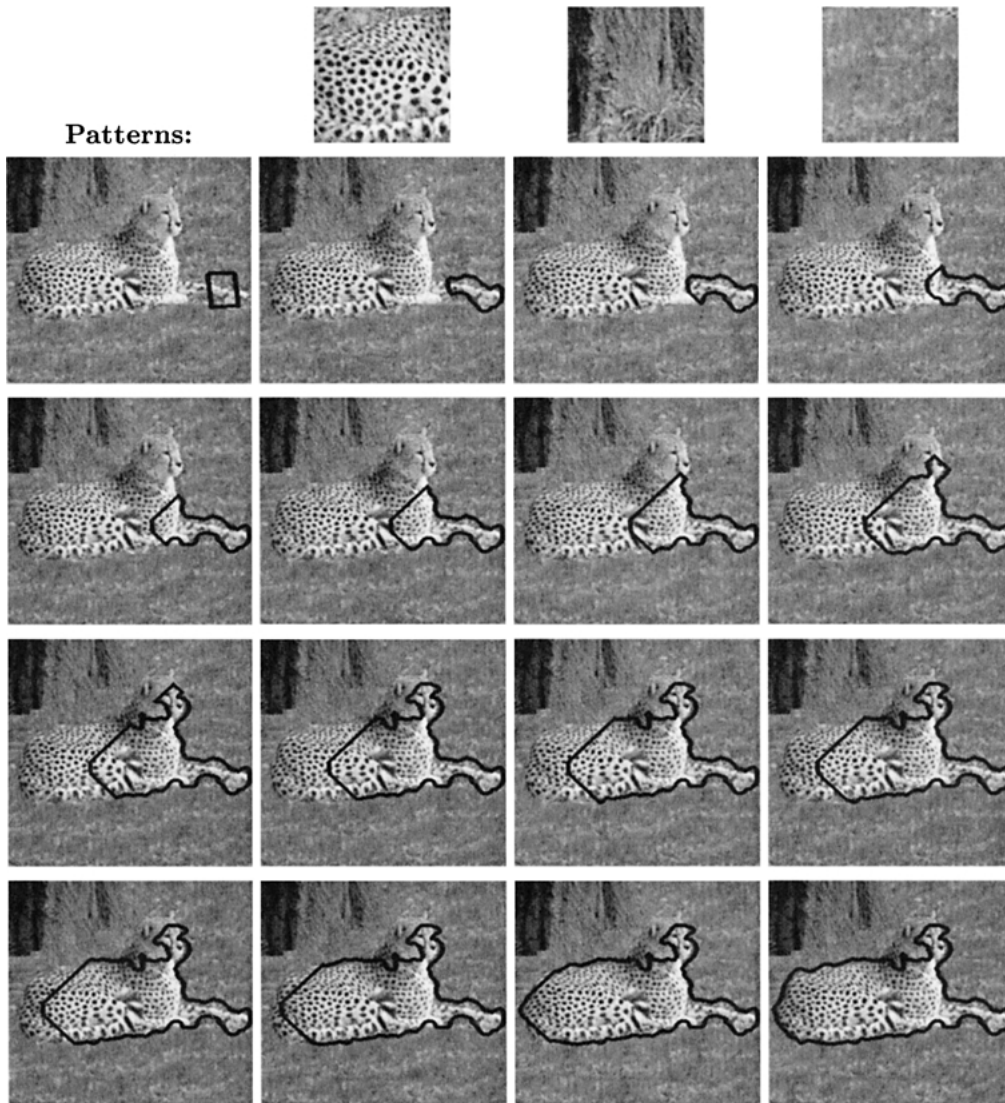


Figure 12. Geodesic Active Regions of supervised texture segmentation. The task of the extraction of a specific region of interest is considered for a real image (chita).

Active Regions model is demonstrated using two different contour initializations.

Finally, the computational cost of our approach is related with the initialization step and for a  $256 \times 256$  frame varies between 2 and 10 seconds (the learning phase is not included) using an ULTRA 10, 299 MHz.

### 5.2. Discussion and Summary

Summarizing, in this paper we have proposed a new framework to deal with frame partition problems in

Computer Vision by the propagation of curves that integrates boundary and region-based frame partition modules under a very general form.

This framework was used as basis to provide a contour propagation method for supervised texture segmentation, that *combines the existing approaches* in the domain of *texture analysis* as well as in the domain of *texture segmentation*.

The main contributions of our approach are:

- A general variational framework is proposed namely the *Geodesic Active Regions*, inspired by the

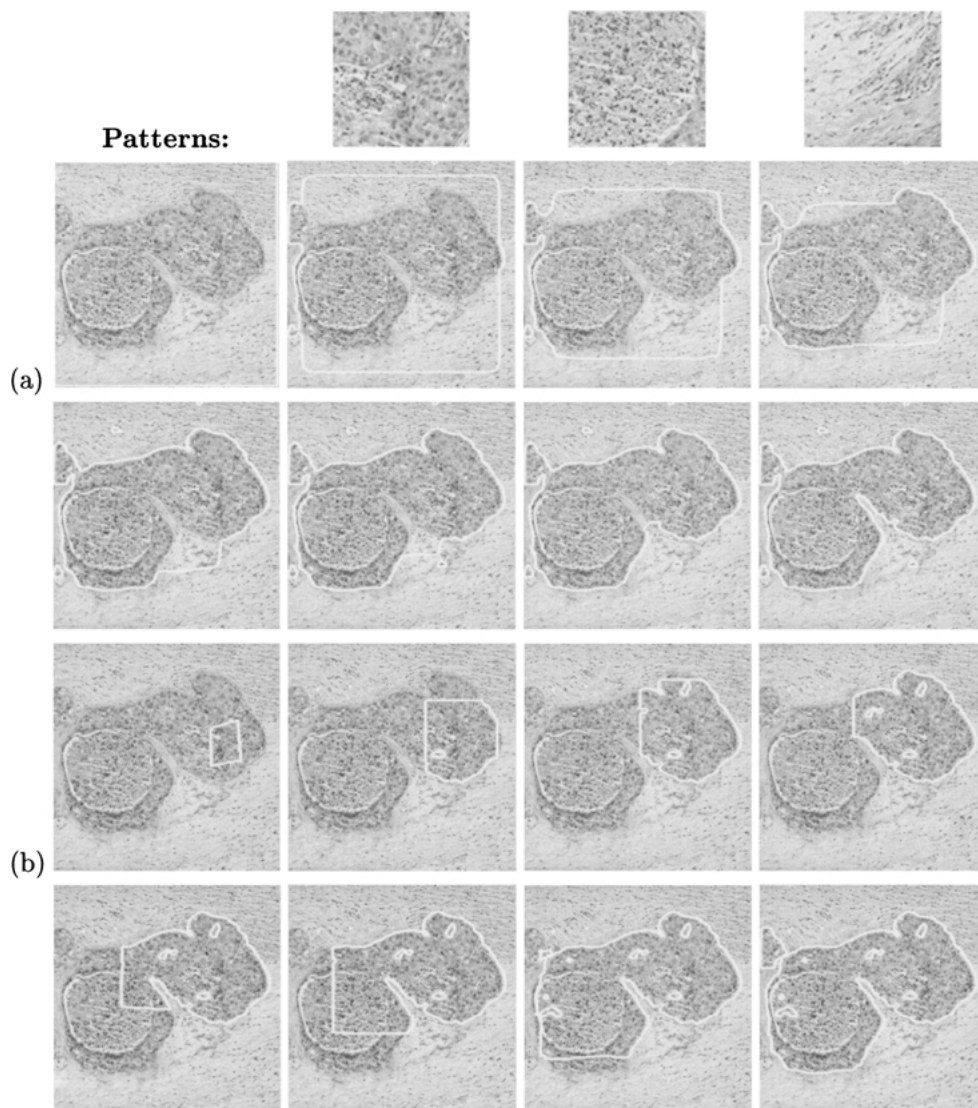


*Figure 13.* Geodesic Active Regions of supervised texture segmentation. The task of segmentation is considered (separation between the background texture region and the others) for a real image (Carcinoma).

- Geodesic Active Contours model which integrates boundary and region-based information modules under a curve-based variational functional,
- The minimization of this functional connects the optimization problem with the propagation of regular curves, which is implemented using the level set theory, a very elegant tool that provides numerous advantages and is free from the initial conditions,
  - A “limited” supervised texture segmentation approach that
- Creates very compact, simple and powerful texture descriptors by combining filtering theory and statistical modeling,
  - Integrates boundary and region-based texture segmentation modules resulting to a robust and flexible model that is independent from the initial conditions,
  - Makes use of the latest developments on the curve evolution theory, and the level set framework which enables numerous advantages (i.e. changes of topology, etc.),

The proposed framework is not limited to texture segmentation, but it can be used to deal with a wide variety of computer vision applications that can be reformulated as frame partition problems.

The future direction of this work is to validate the proposed model using other computer vision problems (Paragios, 2000). Also the incorporation of shape priors to the model is a challenging perspective (Leventon et al., 2000; Chen et al., 2001; Rousson, 2001). Moreover, the acceleration of the proposed method using advanced numerical approximation techniques has to be considered (Weickert et al., 1998; Goldenberg et al., 1999).

Various experimental results (in MPEG format), including the ones shown in this article, can be found at: <http://www.inria.fr/robotvis/personnel/nparagios/demos/>

## Note

1. These methods combined with level set representations (Osher and Sethian, 1988; Sethian, 1996; Osher and Fedkiw, 2000) have been increasingly considered by the Computer Vision community to deal with a variety of problems and applications like segmentation, registration, restoration, 3D reconstruction, shape from shading, motion estimation, tracking, image inpainting, etc. (Caselles et al., 1995; Kimmel and Bruckstein, 1995; Tek and Kimia, 1995; Deriche and Faugeras, 1996; Zhao et al., 1996; Bertalmio et al., 1998; Faugeras and Keriven, 1998; Kornprobst et al., 1998; Malladi and Sethian, 1998; Lorigo et al., 2000; Jehan-Besson et al., 2001; Sapiro, 2001; Sifakis et al., 2001; VLISM, 2001).

## References

- Adalsteinsson, D. and Sethian, J. 1995. A fast level set method for propagating interfaces. *Journal of Computational Physics*, 118:269–277.
- Adams, R. and Bischof, L. 1994. Seeded region growing. *IEEE Transactions on Pattern Analysis and Machine Intelligence*, 16:641–647.
- Amadiou, O., Debreuve, E., Barlaud, M., and Aubert, G. 1999. Inward and outward curve evolution using level set method. In *IEEE International Conference on Image Processing*, Vol. III, pp. 188–192.
- Bertalmio, M., Sapiro, G., and Randall, G. 1998. Morphing active contours: A geometric approach to topology independent image segmentation and tracking. In *IEEE International Conference on Image Processing*, pp. 318–322.
- Blake, A. and Isard, M. 1997. *Active Contours*. Springer-Verlag: Berlin.
- Bouman, C. and Liu, B. 1991. Multiple resolution segmentation of textured images. *IEEE Transactions on Pattern Analysis and Machine Intelligence*, 13:99–113.
- Bovik, A., Clark, M., and Geister, W. 1990. Multichannel texture analysis using localized spatial filters. *IEEE Transactions on Pattern Analysis and Machine Intelligence*, 12:55–73.
- Canny, J. 1986. A computational approach to edge detection. *IEEE Transactions on Pattern Analysis and Machine Intelligence*, 8:769–798.
- Caselles, V., Kimmel, R., and Sapiro, G. 1995. Geodesic active contours. In *IEEE International Conference in Computer Vision*, Boston, USA, pp. 694–699.
- Caselles, V., Kimmel, R., and Sapiro, G. 1997. Geodesic active contours. *International Journal of Computer Vision*, 22:61–79.
- Chakraborty, A., Staib, H., and Duncan, J. 1996. Deformable boundary finding in medical images by integrating gradient and region information. *IEEE Transactions on Medical Imaging*, 15(6):859–870.
- Chan, T. and Vese, L. 1999. An active contour model without edges. In *International Conference on Scale-Space Theories in Computer Vision*, pp. 141–151.
- Chan, T. and Vese, L. 2001. A level set algorithm for minimizing the Mumford-Shah functional in image processing. In *IEEE Workshop on Variational and Level Set Methods*, pp. 161–168.
- Chang, T. and Kuo, C. 1993. Texture analysis and classification with tree-structured wavelet transform. *IEEE Transactions on Image Processing*, 2:429–441.
- Chen, J.-L. and Kundu, A. 1995. Unsupervised texture segmentation using multichannel decomposition and hidden markov models. *IEEE Transactions on Image Processing*, 4:603–619.
- Chen, P. and Pavlidis, T. 1979. Segmentation by texture using co-occurrences matrixes and split-and-merge algorithm. *CVGIP: Image Understanding*, 10:172–182.
- Chen, P. and Pavlidis, T. 1983. Segmentation by texture using correlation. *IEEE Transactions on Pattern Analysis and Machine Intelligence*, 5:64–69.
- Chen, Y., Thiruvenkadam, H., Tagare, H., Huang, F., and Wilson, D. 2001. On the incorporation of shape priors into geometric active contours. In *IEEE Workshop on Variational and Level Set Methods*, pp. 145–152.
- Cohen, L. 1991. On active contour models and balloons. *CVGIP: Image Understanding*, 53:211–218.
- Cross, G. and Jain, A. 1983. Markov random field texture models. *IEEE Transactions on Pattern Analysis and Machine Intelligence*, 5:25–39.
- DeBonet, J. and Viola, P. 1998. Texture recognition using a non-parametric multi-scale statistical model. In *IEEE Conference on Computer Vision and Pattern Recognition*, Santa Barbara, USA, pp. 641–647.
- Deriche, R. 1987. Using Canny's criteria to derive a recursively implemented optimal edge detector. *International Journal of Computer Vision*, 1:167–187.
- Deriche, R. and Faugeras, O. 1996. Les EDP en traitement des images et vision par ordinateur. *Traitement du Signal*, 13. <ftp://ftp-robotvis.inria.fr/pub/html/Papers/deriche-faugeras:96b.ps.gz>.
- Derin, H. and Eliot, H. 1987. Modeling and segmentation of noisy and textured images using Gibbs random fields. *IEEE Transactions on Pattern Analysis and Machine Intelligence*, 9:39–55.
- Duda, R. and Hart, P. 1973. *Pattern Classification and Scene Analysis*. John Wiley & Sons: New York.
- Dunn, D. and Higgins, W. 1995. Optimal Gabor filters for texture segmentation. *IEEE Transactions on Image Processing*, 4:947–964.

- Elfadel, I. and Picard, R. 1994. Gibbs random fields, co-occurrences and texture modeling. *IEEE Transactions on Pattern Analysis and Machine Intelligence*, 16:24–37.
- Faugeras, O. and Keriven, R. 1998. Variational principles, surface evolution, PDE's, level set methods and the stereo problem. *IEEE Transactions on Image Processing*, 7:336–344.
- Gabor, D. 1946. Theory of communications. *IEEE Proceedings*, 93.
- Geman, S. and Geman, D. 1984. Stochastic relaxation, Gibbs distributions, and the Bayesian restoration of images. *IEEE Transactions on Pattern Analysis and Machine Intelligence*, 6:721–741.
- Goldenberg, R., Kimmel, R., Rivlin, E., and Rudzsky, M. 1999. Fast geodesic active contours. In *International Conference on Scale-Space Theories in Computer Vision*, pp. 34–45.
- Gomes, J. and Faugeras, O. 2000. Reconciling distance functions and level sets. *Journal of Visual Communication and Image Representation*, 11:209–223.
- Greenspan, H., Goodman, R., Chellapa, R., and Anderson, C. 1994. Learning texture-discrimination rules in a multi-resolution system. *IEEE Transactions on Pattern Analysis and Machine Intelligence*, 16:894–901.
- Haddon, J. and Boyce, J. 1990. Image segmentation by unifying region and boundary information. *IEEE Transactions on Pattern Analysis and Machine Intelligence*, 12:929–948.
- Jain, A. and Bhattacharjee, S. 1992. Text segmentation using Gabor filters for automatic document processing. *Machine Vision and Applications*, 5:169–184.
- Jain, A. and Farokhnia, F. 1991. Unsupervised texture segmentation using Gabor filters. *Pattern Recognition*, 24:1167–1186.
- Jehan-Besson, S., Barlaud, M., and Aubert, G. 2001. Video object segmentation using Eulerian region based active contours. In *IEEE International Conference in Computer Vision*. Vol. I, Vancouver, Canada, pp. 353–360.
- Jones, G. 1994. Image segmentation using texture boundary detection. *Pattern Recognition Letters*, 15:533–541.
- Kapur, T., Beardsley, P., Gibson, S., Grimson, E., and Wells, W. 1998. Model based segmentation of clinical knee MRI. In *Workshop on Model-based 3-D Image Analysis (in conjunction with ICCV'98)*, Bombay, India.
- Kass, M., Witkin, A., and Terzopoulos, D. 1988. Snakes: Active contour models. *International Journal of Computer Vision*. 1:321–332.
- Khotanzand, A. and Chen, J. 1989. Unsupervised segmentation of textured images by edge detection. *IEEE Transactions on Pattern Analysis and Machine Intelligence*, 13:414–421.
- Kichenassamy, S., Kumar, A., Olver, P., Tannenbaum, A., and Yezzi, A. 1995. Gradient flows and geometric active contour models. In *IEEE International Conference in Computer Vision*. Boston, USA, pp. 810–815.
- Kimmel, R. and Bruckstein, A. 1995. Tracking level sets by level sets: A method for solving the shape from shading problem. *Computer Vision and Image Understanding*, 62:47–58.
- Kornprobst, P., Deriche, R., and Augert, G. 1998. Image sequence restoration: A PDE coupled method for image restoration and motion segmentation. In *European Conference on Computer Vision*. Freighburg, Germany.
- Laine, A. and Fan, J. 1993. Texture classification by wavelet packet signatures. *IEEE Transactions on Pattern Analysis and Machine Intelligence*, 15:1186–1191.
- Leonardis, A., Gupta, A., and Bajcsy, R. 1995. Segmentation of range images as the search for geometric parametric models. *International Journal of Computer Vision*, 14(3):253–270.
- Leventon, M., Grimson, E., and Faugeras, O. 2000. Statistical shape influence in geodesic active contours. In *IEEE Conference on Computer Vision and Pattern Recognition*, pp. I:316–322.
- Lorigo, L., Faugeras, O., Grimson, W., Keriven, R., and Kikinis, R. 1998. Segmentation of bone in clinical knee MRI using texture-based geodesic active contours. In *Medical Image Computing and Computer-Assisted Intervention*, pp. 1195–1204.
- Lorigo, L., Faugeras, O., Grimson, E., Keriven, R., Kikinis, R., Nabavi, A., and Westin, C. 2000. Codimension-two geodesic active contours for the segmentation of tubular structures. In *IEEE Conference on Computer Vision and Pattern Recognition*, pp. I:444–451.
- Ma, W. and Manjunath, B. 1997. Edge flow: A framework for boundary detection and image segmentation. In *IEEE Conference on Computer Vision and Pattern Recognition*. Puerto Rico, USA, pp. 744–749.
- Malladi, R. and Sethian, J. 1998. A real-time algorithm for medical shape recovery. In *IEEE International Conference in Computer Vision*. Bombay, India, pp. 304–310.
- Malladi, R., Sethian, J., and Vemuri, B. 1995. Shape modeling with front propagation: A level set approach. *IEEE Transactions on Pattern Analysis and Machine Intelligence*, 17:158–175.
- Mallat, S. 1989. Multiresolution approximations and wavelet orthonormal bases of  $L^2(R)$ . *Trans. Amer. Math. Soc.*, 315:69–87.
- Manjunath, B. and Chellapa, R. 1991a. A computational approach to boundary detection. In *IEEE Conference on Computer Vision and Pattern Recognition*, pp. 358–362.
- Manjunath, B. and Chellapa, R. 1991b. Unsupervised texture segmentation using Markov random field models. *IEEE Transactions on Pattern Analysis and Machine Intelligence*, 13:478–482.
- Mao, J. and Jain, A. 1992. Texture classification and segmentation using multiresolution simultaneous autoregressive models. *Pattern Recognition*, 25:173–188.
- Mumford, D. and Shah, J. 1985. Boundary detection by minimizing functionals. In *IEEE Conference on Computer Vision and Pattern Recognition*. San Francisco, USA, pp. 22–26.
- Osher, S. and Fedkiw, R. 2000. Level set methods. Technical Report CAM-00-08, Mathematics Department, UCLA. <ftp://ftp.math.ucla.edu/pub/camreport/cam00-08.ps.gz>.
- Osher, S. and Sethian, J. 1988. Fronts propagating with curvature-dependent speed: Algorithms based on the Hamilton-Jacobi formulation. *Journal of Computational Physics*, 79:12–49.
- Panjawani, D. and Healey, G. 1995. Markov random field models for unsupervised segmentation of textured color images. *IEEE Transactions on Pattern Analysis and Machine Intelligence*, 17:939–954.
- Paragios, N. 2000. Geodesic active regions and level set methods: Contributions and applications in artificial vision. Ph.D. Thesis, School of Computer Engineering, University of Nice/Sophia Antipolis. <http://www.inria.fr/RRRT/TU-0636.html>.
- Paragios, N. and Deriche, R. 1999a. Geodesic active contours for supervised texture segmentation. In *IEEE Conference on Computer Vision and Pattern Recognition*. Colorado, USA, pp. II:422–427.
- Paragios, N. and Deriche, R. 1999b. Geodesic active regions for supervised texture segmentation. In *IEEE International Conference in Computer Vision*. Corfu, Greece, pp. 926–932.

- Previous: INRIA Research Report, RR 3440, June 1998, <http://www.inria.fr/RRRT/RR-3440.html>.
- Paragios, N. and Deriche, R. 1999c. Geodesic active regions for motion estimation and tracking. In *IEEE International Conference in Computer Vision*. Corfu, Greece, pp. 688–674.
- Paragios, N. and Deriche, R. 1999d. Unifying boundary and region-based information for geodesic active tracking. In *IEEE Conference on Computer Vision and Pattern Recognition*. Colorado, USA, pp. II:300–305.
- Paragios, N. and Deriche, R. 2000a. Coupled geodesic active regions for image segmentation: A level set approach. In *European Conference in Computer Vision*. Dublin, Ireland, pp. II:224–240. Previous: INRIA Research Report, RR 3783, Oct. 1999, <http://www.inria.fr/RRRT/RR-3783.html>.
- Paragios, N. and Deriche, R. 2000b. Geodesic active contours and level sets for the detection and tracking of moving objects. *IEEE Transactions on Pattern Analysis and Machine Intelligence*, 22:266–280.
- Paragios, N., Mellina-Gottardo, O., and Ramesh, V. 2001. Gradient vector flow fast geodesic active contours. In *IEEE International Conference in Computer Vision*. Vancouver, Canada, pp. I:67–73.
- Pentland, A. 1990. Automatic extraction of deformable part models. *International Journal of Computer Vision*, pp. 107–126.
- Raafat, M. and Wong, C. 1988. Texture information-directed region growing algorithm for image segmentation and region classification. *CVGIP: Image Understanding*, 43:1–21.
- Raghu, D. and Yegnanarajana, B. 1996. Segmentation of Gabor-filtered textures using deterministic relaxation image processing. *IEEE Transactions on Image Processing*, 5:1625–1636.
- Reed, R., Wechsler, H., and Werman, M. 1990. Texture segmentation using a diffusion region growing technique. *Pattern Recognition*, 23:953–960.
- Rousson, M. 2001. Integrating boundary, region, anatomical and shape constraints for medical image segmentation: A level set approach. Master's Thesis, Ecole Supérieure en Sciences Informatique, Nice, France.
- Samson, C., Blanc-Feraud, L., Aubert, G., and Zerubia, J. 1999. A level set model for image classification. In *International Conference on Scale-Space Theories in Computer Vision*, pp. 306–317. <http://www.inria.fr/RRRT/RR-3662.html>.
- Sapiro, G. 1996. Vector-valued active contours. In *IEEE Conference on Computer Vision and Pattern Recognition*, pp. 680–685.
- Sapiro, G. 2001. *Geometric Partial Differential Equations in Image Processing*. Cambridge University Press: Cambridge.
- Sethian, J. 1996. *Level Set Methods*. Cambridge University Press: Cambridge.
- Siddiqi, K., Lauziere, Y.-B., Tannenbaum, A., and Zucker, S. 1997. Area and length minimizing flows for shape segmentation. In *IEEE Conference on Computer Vision and Pattern Recognition*, Puerto Rico, USA, pp. 621–627.
- Sifakis, E., Garcia, C., and Tziritas, G. 2001. Bayesian level sets for image segmentation. *Journal of Visual Communication and Image Representation*, to appear.
- Simoncelli, P., Freeman, W., Adelson, H., and Heeger, H.J. 1992. Shiftable multiscale transforms. Shiftable multiscale transforms: Or what's wrong with orthonormal wavelets. *IEEE Transactions on Information Theory*, 38:587–607.
- Solloway, S., Hutchinson, C., Waterton, J., and Taylor, C. 1997. The use of active shape models for making thickness measurements of articular cartilage from MR images. *MRM*, 37:943–952.
- Tek, H. and Kimia, B. 1995. Image segmentation by reaction-diffusion bubbles. In *IEEE International Conference in Computer Vision*, Boston, USA, pp. 156–162.
- Tsai, A., Yezzi, A., and Willsky, A. 2000. A curve evolution approach to smoothing and segmentation using the Mumford-Shah functional. In *IEEE Conference on Computer Vision and Pattern Recognition*, pp. I:119–124.
- Tsitsiklis, J. 1995. Efficient algorithms for globally optimal trajectories. *IEEE Transactions on Automatic Control*, 40:1528–1538.
- Unser, M. 1986. Local linear transforms for texture measurements. *Signal Processing*, 11:61–79.
- Unser, M. 1995. Texture classification and segmentation using wavelet frames. *IEEE Transactions on Image Processing*, 4:1549–1560.
- VLSM 2001. In *1st IEEE Workshop on Variational and Level Set Methods in Computer Vision*. O. Faugeras, S. Osher, N. Paragios, and J. Sethian (Eds.). Computer Society, Vancouver, Canada, July 01.
- Weickert, J., Haar Romeny, B.M.T., and Viergener, M. 1998. Efficient and reliable scheme for non-linear diffusion and filtering. *IEEE Transactions on Image Processing*, 7:398–410.
- Wu, Y., Zhu, S., and Liu, X. 1999. The equivalence of Julesz ensemble and Gibbs ensemble. In *IEEE International Conference in Computer Vision*, pp. 1025–1032.
- Xu, C. and Prince, J. 1997. Gradient vector flow: A new external force for snakes. In *IEEE Conference on Computer Vision and Pattern Recognition*. Puerto Rico, USA, pp. 66–71.
- Yezzi, A., Tsai, A., and Willsky, A. 1999. A statistical approach to snakes for bimodal and trimodal imagery. In *IEEE International Conference in Computer Vision*. Corfu, Greece, pp. 898–903.
- Yhann, S. and Young, T. 1995. Boundary localization in texture segmentation. *IEEE Transactions on Image Processing*, 4:849–856.
- Zeng, X., Staib, L., Schukz, R., and Duncan, J. 1998. Volumetric layer segmentation using coupled surfaces propagation. In *IEEE Conference on Computer Vision and Pattern Recognition*. Santa Barbara, USA, pp. 708–715.
- Zhao, H.-K., Chan, T., Merriman, B., and Osher, S. 1996. A variational level set approach to multiphase motion. *Journal of Computational Physics*, 127:179–195.
- Zhu, S. 1996. Statistical and computational theories for image segmentation, texture modeling and object recognition. Ph.D. Thesis, Harvard University, USA.
- Zhu, S., Wu, Y., and Mumford, D. 1998. Filters, random field and maximum entropy: Towards a unified theory for texture modeling. *International Journal of Computer Vision*, 27: 1–20.
- Zhu, S. and Yuille, A. 1996. Region competition: Unifying snakes, region growing, and Bayes/MDL for multiband image segmentation. *IEEE Transactions on Pattern Analysis and Machine Intelligence*, 18:884–900.